The Inverse EEG and MEG Problems: The Adjoint State Approach I: The Continuous Case

Olivier Faugeras, François Clément, Rachid Deriche, Renaud Keriven, Théodore Papadopoulo, Jean Roberts, Thierry Viéville, Frédéric Devernay, José Gomes, Gerardo Hermosillo, et al.

INRIA

INSTITUT NATIONAL DE RECHERCHE EN INFORMATIQUE ET EN AUTOMATIQUE

The inverse EEG and MEG problems: The adjoint state approach I: The continuous case

O. Faugeras — F. Clément — R. Deriche — R. Keriven — T. Papadopoulo — J. Roberts — T. Viéville — F. Devernay — J. Gomes — G. Hermosillo — P. Kornprobst — D. Lingrand

N° 3673

Mai 1999

THÈMES 3 et 4

ISSN 0249-6399

SOPHIA ANTIPOLIS

The inverse EEG and MEG problems: The adjoint state approach I: The continuous case

O. Faugeras* , F. Clément† , R. Deriche* , R. Keriven‡ , T. Papadopoulo* , J. Roberts§ , T. Viéville* , F. Devernay¶ , J. Gomes* , G. Hermosillo* , P. Kornprobst* , D. Lingrand*

Thèmes 3 et 4 — Interaction homme-machine,
images, données, connaissances — Simulation et optimisation
de systèmes complexes
Projets Estime, Ondes, Robotvis, Cermics

Rapport de recherche n° 3673 — Mai 1999 — 29 pages

Abstract: In this report, we study the problem of the three-dimensional reconstruction of the electrical activity of the brain from electroencephalography (EEG) and magnetoencephalography (MEG). We use a variational approach based upon three main methods and ideas. The first one is the optimal control of systems governed by elliptic partial differential equations, the second is the regularization of the solutions while preserving the discontinuities (the edges), and the third one is the use of geometric information obtained from magnetic resonance images (MRI) to constrain the solutions in an anatomically "reasonable" way.

Key-words: Electroencephalography, EEG, Magnetoencephalography, MEG, Magnetic Resonance Images, Elliptic partial differential equations, inverse problems, regularisation, measure of brain activity

* Projet Robotvis
† Projet Estime
‡ Cermics
§ Projet Ondes
¶ Société ISTAR
This work was partially supported by the INRIA "Action de Recherche Coopérative" 3D-MEG

Unité de recherche INRIA Sophia Antipolis
2004, route des Lucioles, B.P. 93, 06902 Sophia Antipolis Cedex (France)
Téléphone : 04 92 38 77 77 - International : +33 4 92 38 77 77 —Fax : 04 92 38 77 65 - International : +33 4 92 38 77 65

Problèmes inverses en EEG et MEG : méthode de l'état adjoint I : le cas continu

Résumé : Dans ce rapport, nous étudions le problème de la reconstruction tridimensionnelle de l'activité électrique cérébrale à partir de mesures d'électroencéphalographie (EEG) et de magnétoencéphalographie (MEG). L'approche proposée est variationnelle. Elle utilise trois types de méthodes et d'idées. La première est le contrôle optimal de systèmes gouvernés par des équations aux dérivées partielles elliptiques, la seconde est la régularisation des solutions avec préservation des discontinuités (les contours) et la troisième celle de l'utilisation d'information géométrique issue d'imagerie par résonance magnétique (IRM) pour contraindre les solutions de manière "raisonnable" anatomiquement.

Mots-clés : Électroencéphalographie, EEG, Magnétoencephalographie, MEG, Imagerie par Résonance Magnétique, Équations aux dérivées partielles elliptiques, problèmes inverses, régularisation, mesure de l'activité cérébrale

1 Introduction

Electro-Encephalo-Graphy (EEG) and Magneto-Encephalo-Graphy (MEG) are two noninvasive means of measuring some of the electrical activity of the brain. These techniques are fairly recent: Hans Berger, a German neuropsychiatrist, recorded in 1929 the first human EEG while the first measurements of the magnetic field induced by the brain's electrophysiological events were performed in 1968 by D. Cohen [7] at MIT. The next major advance in biomagnetic technology was the development and successful testing in 1969 of the SQUID (superconducting quantum interference device) by Zimmerman and colleagues [48]. Operating at liquid helium temperatures, the SQUID achieved an unprecedented sensitivity to weak magnetic fields.

These two techniques have found many clinical applications which are reviewed in chapters 8 and 9 of [38]. From the outset researchers have been concerned with the problem of relating the measurements (electric potentials for EEG, magnetic fields for MEG) to the spatiotemporal distribution of the cerebral current sources, a problem known as the inverse EEG or MEG problem. This problem is made difficult by the fact that the relationship between the distribution of current sources and the electromagnetic field is not one to one. For example, it has been known since the time of Helmholtz that there are current distributions which are either magnetically or electrically silent, or both, outside the conductor [23]. This is an indication of the fact that the solution to the inverse problem is not unique. Other difficulties are the high level of noise in the measurements and the small number of measures, though this last problem has tended to be less severe with the advent of new systems with more sensors [22]. Nonetheless this is an indication of the fact that the inverse problem is also ill-posed: small variations in the measurements due to noise may cause unwieldy variations of the solution. This can be partially combated by regularization techniques [4, 37, 11, 3].

Another serious difficulty is the modelling (physical and geometric) of the electrical effects that supposedly give rise to the measurements. Concerning physical modelling, we will see in Section 2 that these effects are due to the electrical activity of some populations of neural cells and in Section 3 that this activity can be (coarsely) modelled by assuming a distribution of conductivities and of primary source currents in the head. In the inverse EEG and MEG problems, one usually assumes that the distribution of conductivities is known but this is usually a gross approximation. As for the geometrical modelling, it is only recently [10, 3, 33], and because of the availibility of Magnetic Resonance Images (MRI) that anatomical constraints, making use of the actual shapes of the head, skull, and brain have been taken into account, e.g. to constrain the position and orientation of the estimated primary source currents. Sophisticated image processing and segmentation algorithms can be applied to the MRI data to extract detailed volume and surface models [46] of the persons' head prior to recording their activity through EEG or/and MEG measurements. Despite the use of these constraints, the spatial resolution of the reconstructed activity (the primary source currents) remains poor compared with what is judged to be acceptable (of the order of 5mm). On the other hand, the temporal resolution is of the order of 1ms and considered to be more than what is needed for functional studies (of the order of 5ms). This is in contrast to other functional brain imaging techniques such as position emission tomography (PET), single photon computed tomography (SPECT) and functional MRI (f-MRI) which have acceptable spatial resolutions but unacceptable time resolutions (1mn in PET/SPECT and 1s in f-MRI).

2 Neural origin of the brain electromagnetic fields.

The brain is the most complex organized structure known to exist; we can convince ourselves of this by examining the following numbers. There are approximately 10^{12} neurons in the central nervous system with at least 10^{10} in the outermost cortical layer. Moreover there are roughly 10^{15} synaptic connections between these neurons that use more than 10^{18} chemical neuro-transmitters/second each built of complex amino-acid chains. This means that approximately 10^{24} elementary molecules/second are contributing to the brain activity. Even though we do not adhere to the simplistic view that the brain is a computer, the comparison is interesting. Let us assume that each molecule "carries" one bit of "information" (note the quotes), then we have to think in terms of a machine capable of processing 10^{12} giga-bits/second, weighing $1-2\ Kg$ and consuming less than $10-15\ Watts$!

Furthermore, this "topographical" complexity is complemented by the fact that the human brain has a very long "history": it is the result of an evolution process which probably started over 200 million years ago

[6]. It is also most of the time in interaction with a complex and variable environment from which it receives of the order of $10^8 - 10^{12}$ bits of information/second.

These numbers point to the fact that only "*macroscopic*" models of such an intricate system can be considered. Moreover, since each neuron is connected to $10^3 - 10^4$ other neurons in the central nervous system individual neuron activity, cannot be considered alone as a relevant indicator of the brain activity. Thus we are pushed again into considering *macroscopic* models of the brain behavior as means of capturing some aspects of its functioning. It turns out that MEG and EEG do capture some macroscopic properties of the brain activity that can hopefully be used to build such models.

We now briefly turn to the biological bases of the electrical activity of the brain which is due to ion mechanisms through the neuron membrane, see figure 1 and [6, 24].

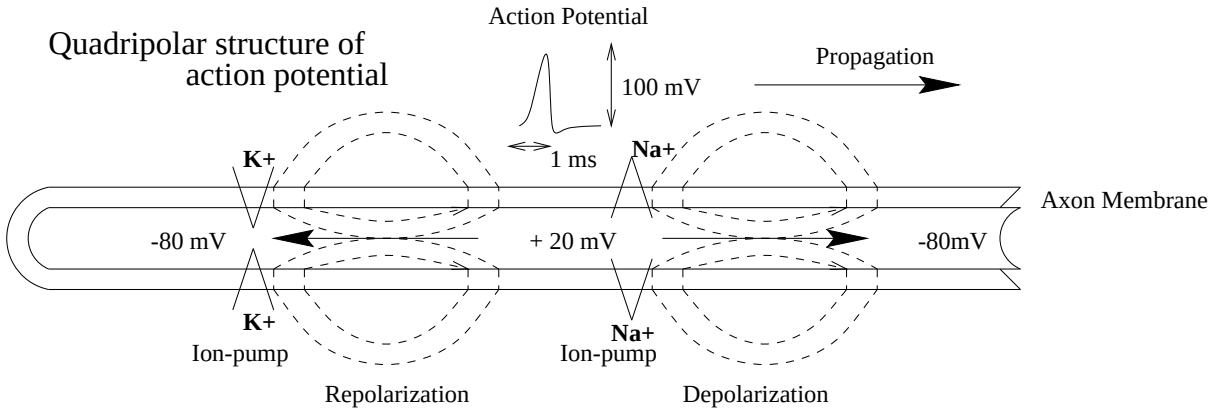

Figure 1: Extracellular current sources and sinks in the axon.

Signal reception In a very simplified manner, when a neuro-transmitter molecule touches a neuron, the membrane permeability is altered for specific ions (Na+ and K+) for which the concentration was originally maintained out of equilibrium by Na-K "pumps" so that they suddenly rush through the membrane and give rise to a *post-synaptic potential* of about $10mV$ with a duration of $10ms$.

The key-point is that this mechanism has a simple geometric structure and can be represented as a *dipolar* field, decreasing as the inverse of the square of the distance.

The related current-dipole moment which models this effect is of the order of $10\,nA\,m$, so that about 10^6 neurons must be activated simultaneously to generate a measurable electro-magnetic field.

With thousands of synapses per neuron (pyramidal cells in fact), and an average density of 10^5 neurons per mm^2, one would expect to be able to detect activations of areas smaller that $1mm^2$, but in practice, because of partial cancellation of the electro-magnetic field, experimental studies (see [22] for a review) show that only activities of areas of $40 - 200mm^2$ are detectable.

Signal emission The second source of electro-magnetic fields is due to *action potential* as detailed in figure 1, when the neuron is propagating a signal along its axon. A similar Na-K "pump" mechanism is at the origin of these currents whose frequency (not amplitude) encodes the neuronal information.

The important point is that this phenomenon is well modeled by a *quadripolar* structure (i.e. two oppositely oriented dipoles whose actions cancel each other) generating a field decreasing as the inverse of the cube of the distance. Its effect is thus negligible with respect to the post-synaptic potential when measured outside the cortex, even if its amplitude is higher.

Furthermore, the time constant of this phenomenon is an order of magnitude smaller ($1ms$) than post-synaptic potentials ($10ms$). It thus contributes to higher-frequency fields which tend to cancel each other when averaged over time.

In summary, even though action-potentials do contribute to the electromagnetic fields outside the head they are not yet measured by current technology in EEG and MEG (contrary to what could be done in the peripheral nervous system).

To refine a little our analysis, it is important to note that not all neurons generate a measurable electromagnetic field. In the central nervous system, because the field generated by dipoles decreases with the inverse of the square of the distance, only currents present in the cortex will be measurable.

Furthermore, not all cortical cells will induce fields measurable through EEG or MEG. For instance stellate cells generate "closed fields" in the sense that their synapses have a homogeneous density because the neuron dendrites which receive the synaptic junctions have ramifications in all directions. Anatomically it is only the *pyramidal cells* (as shown in figure 2.A) which generate a relevant electromagnetic field, since they have a "dipolar" configuration, see figure 2.B. Those cells, mostly present in the 3rd of the 6 cortical

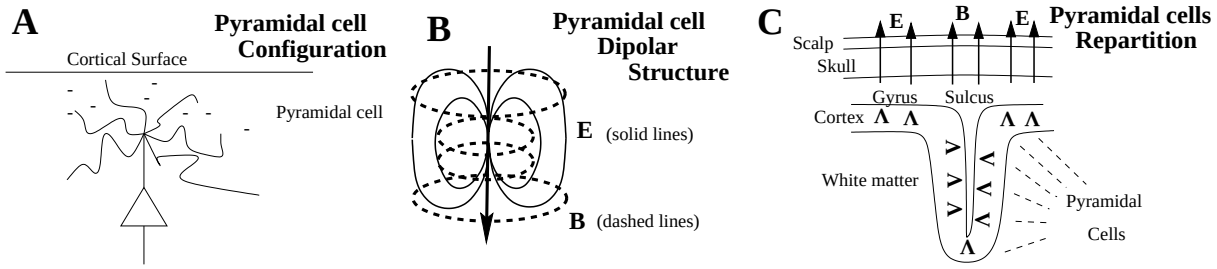

Figure 2: Pyramidal cells in the cortex.

layers for the visual cortex or in the 5th layer (pyramidal Betz cells) of the motor cortex mainly relay "local" information within the different cortical layers and constitute almost 70 % of neo-cortical neurons. They thus yield information about the internal "vertical" activity below the cortex surface in a given cortical column.

Considering that the average behavior of a population of such cells is modeled as an electrical dipole with a normal magnetic field and a tangential electric field (as shown in figure 2.C), we easily deduce that EEG measurements will be mainly related to the activity of these cells in cortical gyri (parallel to the skull) whereas MEG measurements will be mainly related to the activity of these cells in cortical sulci (normal to the skull).

In conclusion, EEG and MEG are complementary measures of some of the cortex electrical activity due to the variations of the post-synaptic potentials of the pyramidal cells in the cortical columns.

3 Macroscopic physical models of brain activity

3.1 Notation.

Vectors and matrixes are denoted in boldface. The vector of $\mathbb{R}^3$ indicating the position of the point r (resp. r') will be denoted $\mathbf{r}$ (resp. $\mathbf{r}'$). ∇ denotes the usual "nabla" operator. It is such that for a real function $f(\mathbf{r})$ (resp. $f(\mathbf{r}')$), ∇f (resp. $\nabla' f$) is the gradient of f, i.e. the vector whose coordinates are the partial derivatives of f with respect to the coordinates of $\mathbf{r}$ (resp. of $\mathbf{r}'$). For a given smooth vector field $\mathbf{X}(\mathbf{r})$ $\nabla \cdot \mathbf{X}$ is the divergence of this field (a scalar) and $\nabla \times \mathbf{X}$ is the curl of this field (a vector).

Given two points r and r', the vector $\mathbf{R} = \mathbf{r} - \mathbf{r}'$ and its norm $R = \|\mathbf{R}\|$ play an important role in the sequel. The function $\frac{1}{R}$ is a function of $\mathbf{r}$ and $\mathbf{r}'$. We can therefore consider its gradient, noted $\nabla\left(\frac{1}{R}\right)$ with respect to $\mathbf{r}$ and its gradient, denoted $\nabla'\left(\frac{1}{R}\right)$, with respect to $\mathbf{r}'$. The relation between the two is straightforward:

$$\nabla'\left(\frac{1}{R}\right) = -\nabla\left(\frac{1}{R}\right) = \frac{\mathbf{R}}{R^3}. \tag{1}$$

3.2 The Maxwell equations.

We start from Maxwell's equations in *a void*:

$$\nabla \cdot \mathbf{E} = \frac{\rho}{\varepsilon_0}, \qquad \nabla \times \mathbf{E} = -\frac{\partial \mathbf{B}}{\partial t} \tag{2}$$

with the *electrical permittivity* $\varepsilon_0 \simeq 8.85\ 10^{-12} F\, m^{-1}$, and

$$\nabla \cdot \mathbf{B} = 0, \qquad \nabla \times \mathbf{B} = \mu_0 \left(\mathbf{J} + \varepsilon_0 \frac{\partial \mathbf{E}}{\partial t} \right) \tag{3}$$

with the *magnetic permeability* $\mu_0 = 4\pi 10^{-7} H\, m^{-1}$. We note that the permeability of tissues in the head is that of empty space, i.e. $\mu = \mu_0$ and that $\varepsilon_0\, \mu_0\, c^2 = 1$, where $c = 3.00\, 10^8\, m\, s^{-1}$ is the velocity of light in a void.

Here, the *charge density* ρ and the *current density* $\mathbf{J}$ are related by

$$\nabla \cdot \mathbf{J} = -\frac{\partial \rho}{\partial t}\,.$$

Furthermore, in a passive (no charge, nor current generator) non-magnetic medium, $\mathbf{J}$ is the sum of the *ohmic volume* current and the *polarization* current, respectively:

$$\mathbf{J} = \sigma\, \mathbf{E} + \frac{\partial \mathbf{P}}{\partial t}\,, \tag{4}$$

where $\mathbf{P} = (\varepsilon - \varepsilon_0)\, \mathbf{E}$ is the polarization and σ (expressed in $\Omega^{-1}\, m^{-1}$) and ε are the conductivity and the permittivity of the material, respectively.

3.3 Quasi-static approximation of the Maxwell equations.

The quasi-static approximation (justified in [22] and appendix A) allows us to neglect all time derivatives in those equations. Since the curl of the electric field $\mathbf{E}$ is zero, that field is the gradient of a potential V:

$$\mathbf{E} = -\nabla V.$$

In the quasi-static approximation, Maxwell's fourth equation becomes

$$\nabla \times \mathbf{B} = \mu_0 \mathbf{J},$$

which, combined with the third equation, implies the Biot-Savart law for computing the magnetic field at any point $\mathbf{r}$ from the current density $\mathbf{J}$:

$$\mathbf{B}(\mathbf{r}) = \frac{\mu_0}{4\pi} \int_\Omega \mathbf{J}(\mathbf{r}') \times \nabla' \left(\frac{1}{R} \right) dr'\,. \tag{5}$$

See appendix A for a review.

3.4 The current-law and the EEG problems.

Although the term $\frac{\partial \mathbf{P}}{\partial t}$ is null in equation (4) using the quasi-static approximation, this current law must be modified because the brain is not a passive medium, but is subject to an electrical activity reflected by a *primary current*, noted $\mathbf{J}^p$. We thus have to write:

$$\mathbf{J}(\mathbf{r}) = \mathbf{J}^p(\mathbf{r}) + \sigma(\mathbf{r})\, \mathbf{E}(\mathbf{r}) = \mathbf{J}^p(\mathbf{r}) - \sigma(\mathbf{r})\, \nabla V(\mathbf{r}) \tag{6}$$

The primary current distribution is precisely what EEG and MEG are trying to estimate.

If we now use the fourth of Maxwell's equation, $\nabla \times \mathbf{B} = \mu_0 \mathbf{J}$, take the divergence of both sides, and use the fact that $\nabla \cdot (\nabla \times \mathbf{B}) = 0$, we obtain a very important equation that connects the primary current $\mathbf{J}^p$, the electric potential V and the conductivity σ:

$$\nabla \cdot (\sigma \nabla V) = \nabla \cdot \mathbf{J}^p . \tag{7}$$

We make use of the relation $\nabla \cdot (\sigma \nabla V) = \nabla \sigma \cdot \nabla V + \sigma \Delta V$ to rewrite this equation:

$$\nabla \sigma \cdot \nabla V + \sigma \Delta V = \nabla \cdot \mathbf{J}^p . \tag{8}$$

The *direct* problem in EEG is that of computing the potential $V(\mathbf{r})$ given the primary current $\mathbf{J}^p(\mathbf{r})$ and the conductivity $\sigma(\mathbf{r})$. The *inverse* problem in EEG is, given measures of the potential V at some points $\mathbf{r}_1, \ldots, \mathbf{r}_{n_V}$, and the conductivity $\sigma(\mathbf{r})$, to estimate the primary current $\mathbf{J}^p(\mathbf{r})$.

3.5 The Biot-Savart law and the MEG problems.

If we now replace the current $\mathbf{J}$ by its value (6) in the Biot-Savart equation (5), we obtain

$$\mathbf{B}(\mathbf{r}) = \mathbf{B}_0(\mathbf{r}) - \frac{\mu_0}{4\pi} \int_\Omega \sigma(\mathbf{r}') \nabla' V \times \nabla' \left(\frac{1}{R} \right) dr', \tag{9}$$

with

$$\mathbf{B}_0(\mathbf{r}) = \frac{\mu_0}{4\pi} \int_\Omega \mathbf{J}^p(\mathbf{r}') \times \nabla' \left(\frac{1}{R} \right) dr' , \tag{10}$$

where $\mathbf{B}_0$ is the magnetic field produced by the primary current $\mathbf{J}^p$, or equivalently

$$\mathbf{B}(\mathbf{r}) = \mathbf{B}_0(\mathbf{r}) + \frac{\mu_0}{4\pi} \int_\Omega V(\mathbf{r}') \nabla' \sigma \times \nabla' \left(\frac{1}{R} \right) dr', \tag{11}$$

as shown in appendix A.2.

Equations (9) and (11) are just as important for MEG as equation (7) is for EEG. Note however that there is a major difference between those equations: while equation (7) is implicit (i.e. allows the computation of V), equations (9) and (11) explicitly define $\mathbf{B}(\mathbf{r})$ in terms of V, σ and $\mathbf{J}^p$. For this reason, equation (7) also plays a fundamental role in the case of MEG and will play the central role in the remainder of this report.

The *direct* problem in MEG is to compute the magnetic field $\mathbf{B}(\mathbf{r})$ given the primary current $\mathbf{J}^p(\mathbf{r})$, and the conductivity $\sigma(\mathbf{r})$ and the potential $V(\mathbf{r})$. It is solved in a straightforward fashion from equations (9) and (11). The *inverse* problem in MEG is, given measures of some components of the magnetic field at some points $\mathbf{q}_1, \ldots, \mathbf{q}_{n_B}$, and the conductivity $\sigma(\mathbf{r})$, to estimate the primary current $\mathbf{J}^p(\mathbf{r})$. Note that this requires the computation of the potential $V(\mathbf{r})$.

In some cases [9, 34, 22, 40], we may have measurements of both the electric potential and some components of the magnetic field. The *inverse* EEG+MEG problem is, given those measurements and the conductivity $\sigma(\mathbf{r})$, to estimate the primary current $\mathbf{J}^p(\mathbf{r})$.

3.6 The surface approach

Our knowledge of the conductivity of the brain tissues is very limited [22]. Therefore, in EEG or MEG studies, it is often assumed that the head is made out of a number n of disjoint homogeneous regions $\Omega_1, \ldots, \Omega_n$ with boundaries $S_1 = \partial\Omega_1, \ldots, S_n = \partial\Omega_n$. Those regions are usually chosen to be the scalp, skull, cerebrospinal fluid, gray matter and white matter. The conductivity $\sigma(\mathbf{r})$ is constant in each of the regions, equal to σ_i in Ω_i, and therefore its gradient, which appears in equations (8) and (11), is nonzero only on the boundaries S_i. This has allowed researchers in the fields of EEG and MEG to replace those equations by simpler ones, involving only surface integrals of the electric potential. An example of typical conductivity values are .33, .0042 and .33 $\Omega^{-1}m^{-1}$ for the scalp, skull and brain respectively [35, 3] (In [30], the human skull phantom has conductivity values of 53, 1 and 100 for scalp, skull and brain respectively).

Concerning the role of anisotropies in the conductivity values, one can refer to [33], where the authors study the influence of skull anisotropy on the forward and inverse problem in EEG and conclude that this influence is important for the forward problem, while the question remains open for the case of the inverse problem.

Before we write these equations, we introduce some notation. If regions Ω_i and Ω_j are adjacent, we denote by S_{ij} their common boundary, i.e. $S_i \cap S_j$. We also denote by $\mathbf{n}_i(\mathbf{r})$ the unit normal vector to S_i at the point $\mathbf{r}$ of S_i *oriented toward the outside* of Ω_i and by $\mathbf{n}_{ij}(\mathbf{r})$ the unit normal vector to S_{ij} at the point $\mathbf{r}$ of S_{ij} also oriented toward the outside of Ω_i. ds_{ij} denotes the area element of S_{ij}. Surface elements referring to integration with respect to the variable $\mathbf{r}$ (resp. $\mathbf{r}'$) will be denoted by ds (resp. ds').

It is known ([18] and appendix B) that equation (8) for the potential becomes

$$\mathbf{r} \in S_{ij} \Rightarrow (\sigma_i + \sigma_j)\, V(\mathbf{r}) = 2\sigma_0 V_0(\mathbf{r}) - \frac{1}{2\pi} \sum_{kl} (\sigma_k - \sigma_l) \int_{S_{kl}} V(\mathbf{r}')\, \nabla' \left(\frac{1}{R}\right) \cdot \mathbf{n}_{kl}(\mathbf{r}')\, ds'_{kl}\,. \tag{12}$$

The sum is taken over all pairs of adjacent regions S_k and S_l. V_0 is defined by

$$V_0(\mathbf{r}) = \frac{1}{4\pi\sigma_0} \int_\Omega \nabla' \left(\frac{1}{R}\right) \cdot \mathbf{J}^p(\mathbf{r}')\, dr' = -\frac{1}{4\pi\sigma_0} \int_\Omega \frac{\nabla' \cdot \mathbf{J}^p}{R} dr'\,, \tag{13}$$

where $\sigma_0 = 1$. V_0 is the potential due to the primary current $\mathbf{J}^p$ in a medium of unit conductivity.

Note that equation (12) is of the form

$$f(V) + U_0 = \lambda V\,,$$

with $U_0 = 2\sigma_0 V_0$, $\lambda = \sigma_i + \sigma_j$ and f is an integral operator:

$$f(V)(\mathbf{r}) = \int_{S=\cup S_{kl}} K(\mathbf{r}, \mathbf{r}') V(\mathbf{r}') ds'\,,$$

where $K(\mathbf{r}, \mathbf{r}') = -\frac{1}{2\pi}(\sigma_k - \sigma_l)\nabla' \left(\frac{1}{R}\right) \cdot \mathbf{n}_{kl}(\mathbf{r}')$ for $\mathbf{r}' \in S_{kl}$. This is a Fredholm integral of the second type [8, 13].

Similarly ([18] and appendix B), equation (11) can be replaced by

$$\mathbf{B}(\mathbf{r}) = \mathbf{B}_0(\mathbf{r}) + \frac{\mu_0}{4\pi} \sum_{kl} (\sigma_k - \sigma_l) \int_{S_{kl}} V(\mathbf{r}')\, \mathbf{n}_{kl}(\mathbf{r}') \times \nabla' \left(\frac{1}{R}\right) ds'_{kl}\,, \tag{14}$$

with $\mathbf{B}_0$ still given by equation (10).

4 The thrust of the paper

The methods that have been proposed for solving the inverse EEG and MEG problems fall into several main categories. The approach can be probabilistic/bayesian including maximum a posteriori estimates [3], maximum-likelihood [20] estimates, or it can be deterministic. It may assume a discrete [47, 41, 42, 36] or distributed [21, 3] source model. In the case of a distributed source model various steps have been taken to regularize the solution by choosing minimum-norm solutions [21, 39] or by limiting the spatial-temporal variation of the solution except at edges [3]. Recently, anatomical and physiological constraints [10, 16, 17, 3] have also been introduced to prevent the solutions from appearing in unrealistic areas of the head.

The thrust of this paper is to propose a new approach for solving the EEG, MEG and EEG+MEG inverse problems in a very general framework. In particular, we do not assume that the conductors involved have special shapes, e.g. spheres, but our framework allows us to incorporate any a priori information concerning those shapes, e.g. information from anatomical MRI, see section 9. We do not assume either that the primary current $\mathbf{J}^p(\mathbf{r})$ is a finite set of dipoles. In fact we assume that it is a general function, but our framework allows us to incorporate any a priori information concerning this current, e.g. that it is localized in the cortex and can have "sharp" edges.

The approach is variational and uses recent advances in computer vision where variational approaches and Partial Differential Equations (PDE's) have been used succesfully to solve a number of difficult problems such as computation of optical flow, restoration, segmentation, stereo [27, 29, 15]. It also borrows from optimal control theory where the estimation of distributed parameters in systems driven by PDE's has received considerable attention in the last thirty years [31, 32, 5].

5 The adjoint state approach

We now give a general description of the method we propose to use in order to solve the inverse EEG, MEG and EEG+MEG problems. We consider a set W of real functions that form a real Hilbert space, i.e. it is a complete normed real vector space with an inner product. In our case, we will consider real square integrable functions defined on an open bounded region Ω equipped with the inner product

$$\langle u,\, v\rangle = \int_\Omega u(\mathbf{r})\, v(\mathbf{r}) dr,$$

which defines the L^2 norm as:

$$\|u\|^2 = \langle u, u\rangle\,.$$

In practice we will have to consider somewhat more complicated functional spaces, such as the Sobolev spaces $H^1(\Omega)$ and $H^1_0(\Omega)$ [44, 32], but we can ignore this difficulty at this level of detail.

Let the vector $\mathbf{p}$ represent a set of parameters which can be scalar or vector functions defined in some functional space, denoted W_3. For any $\mathbf{p}$ in W_3, we consider the (hopefully unique) function v of W which satisfies the state equation

$$\mathbf{A}(\mathbf{p})v = f(\mathbf{p}), \tag{15}$$

where $\mathbf{A}(\mathbf{p})$ is a linear operator from W to another set $W_1 \subset W$ and f is a function of W_1. We rewrite this state equation using a variational formulation,

$$\langle \mathbf{A}(\mathbf{p})v - f(\mathbf{p}), w\rangle = 0 \quad \text{for all} \quad w \quad \text{in} \quad W_2, \tag{16}$$

where the space W_2 for the test functions w depends on the application and is generally related to W.

This defines a mapping $\mathbf{p} \to v(\mathbf{p})$ where the solution $v(\mathbf{p})$ of equations (15) and (16) is called the state function. To give some intuition, in the EEG case the state function v is the electrical potential V and the vector $\mathbf{p}$ is the conductivity $\sigma(\mathbf{r})$ and the primary source current vector $\mathbf{J}^p(\mathbf{r})$. The state equation is either equation (7) or equation (12).

We also make measurements which can be modeled as the application of a linear operator, denoted $\mathbf{M}(\mathbf{p})$, to our state functions v. This operator maps W to $\mathbb{R}^n$. Examples of such operators are given in equations (23) and (24). We define the measurements error functional

$$\mathcal{J}(\mathbf{p}) = \frac{1}{2}\|\mathbf{M}(\mathbf{p})v - \mathbf{m}\|^2, \tag{17}$$

where $\|\cdot\|^2$ is, for example, the usual Euclidean norm in $\mathbb{R}^n$, and $\mathbf{m}$ is a given vector of measurements. The inverse problem of finding the parameter $\mathbf{p}$ that would best reproduce the measurements $\mathbf{m}$ is then defined as the minimization of the error $\mathcal{J}$ with respect to the parameter $\mathbf{p}$. This corresponds to the constrained minimization problem

$$\min_{\mathbf{p}\,\text{in}\,W_3} \mathcal{J}(\mathbf{p}) \quad \text{subject to} \quad v = v(\mathbf{p}) \quad \text{solution of} \quad (15) \quad \text{or} \quad (16). \tag{18}$$

We propose to solve the minimization problem by a descent algorithm using the information on the gradient and we compute the gradient of the error criterion with the adjoint state approach. This amounts to consider Lagrange multipliers which, in this continuous setting, become a function w "living" in the space of test funcions W_2. We form the Lagrangian by adding the error criterion, expressed in terms of the state function, and the constraining state equation, expressed in the variational form:

$$\mathcal{L} = \mathcal{L}(v, w; \mathbf{p}) = \frac{1}{2}\|\mathbf{M}(\mathbf{p})v - \mathbf{m}\|^2 + \langle w, \mathbf{A}(\mathbf{p})v - f(\mathbf{p})\rangle. \tag{19}$$

This Lagrangian is a functional from the cartesian product $W \times W_2 \times W_3$ into $\mathbb{R}$ which we assume to be differentiable. This implies the existence of G-derivatives (G for Gateaux) with respect to all three "coordinates" v, w, $\mathbf{p}$. We remind the reader of the definition of Gateaux- or G-derivative of a functional F from a normed vector space W into $\mathbb{R}$.

Definition 1 *F is G-derivable at $v \in W$ if*

1. *$\forall \delta w \in W$ the limit $\delta F = \lim_{\theta \to 0, \theta \neq 0} \frac{F(v+\theta\delta w)-F(v)}{\theta}$ exists.*
2. *The application $F'(v) : \delta w \to \delta F$ is linear and continuous from W to $\mathbb{R}$ (In the case where F is is differentiable, it is simply its derivative at v).*

As soon as $v = v(\mathbf{p})$ is solution of the state equation, we have

$$\mathcal{J}(\mathbf{p}) = \mathcal{L}(v(\mathbf{p}), w; \mathbf{p}). \tag{20}$$

We assume that the mapping $\mathbf{p} \to v(\mathbf{p})$ is differentiable and take the the G-derivative with respect to $\mathbf{p}$ of both sides of the previous equation. This yields the relation

$$\delta\mathcal{J} = \frac{\partial\mathcal{L}}{\partial v}(v(\mathbf{p}), w; \mathbf{p})\delta v + \frac{\partial\mathcal{L}}{\partial \mathbf{p}}(v(\mathbf{p}), w; \mathbf{p})\delta\mathbf{p} \tag{21}$$

which holds for all w in W_2. We choose the Lagrange multiplier w so that the first term vanishes, i.e. defined by

$$\frac{\partial\mathcal{L}}{\partial v}(v(\mathbf{p}), w; \mathbf{p})\delta v = 0 \quad \text{for all} \quad \delta v.$$

We now use the fact that in a Hilbert space, if $\mathbf{H}$ is a linear operator, the inner product $\langle x, \mathbf{H}y\rangle$ is equal to $\langle \mathbf{H}^* x, y\rangle$, where $\mathbf{H}^*$ is the linear operator adjoint to $\mathbf{H}$.

We thus introduce the two adjoint operators $\mathbf{M}(\mathbf{p})^*$ and $\mathbf{A}(\mathbf{p})^*$ and rewrite the previous equation as

$$\langle \mathbf{M}(\mathbf{p})^*(\mathbf{M}(\mathbf{p})v - \mathbf{m}), \delta v\rangle + \langle \mathbf{A}^*(\mathbf{p})w, \delta v\rangle = 0 \quad \text{for all} \quad \delta v,$$

which is equivalent to

$$\mathbf{A}^*(\mathbf{p})w + \mathbf{M}^*(\mathbf{p})\left(\mathbf{M}(\mathbf{p})v - \mathbf{m}\right) = \mathbf{0}. \tag{22}$$

This equation is called the adjoint state equation.

Therefore, if $v(\mathbf{p})$ and $w(\mathbf{p})$ are respectively solutions of (15) and (22), the relation (21) reduces to

$$\delta\mathcal{J} = \frac{\partial\mathcal{L}}{\partial \mathbf{p}}(v(\mathbf{p}), w; \mathbf{p})\delta\mathbf{p}.$$

Hence the gradient of the error criterion can be computed from the sole derivatives of $\mathbf{M}(\mathbf{p})$, $\mathbf{A}(\mathbf{p})$ and $f(\mathbf{p})$ with respect to $\mathbf{p}$.

To summarize, the minimization problem (18) is solved by the following steps

1. Start from an estimate $\mathbf{p}_0$. Set $i = 0$.
2. Solve the state equation (15) and obtain a solution v_i.
3. Solve the adjoint state equation(22) with this value of v_i and obtain a solution w_i.
4. With those values of v_i and w_i determine the gradient $\frac{\partial\mathcal{J}}{\partial\mathbf{p}}$ at point $\mathbf{p}_i$ and determine a new value $\mathbf{p}_{i+1}$ of $\mathbf{p}$, set $i = i + 1$.
5. If $\mathbf{p}_{i+1}$ is significantly different from $\mathbf{p}_i$ then go to 2, else stop.

The previous discussion shows that the main advantage of the adjoint state method is to reduce the cost of the computation of the derivative $\frac{\partial\mathcal{J}}{\partial\mathbf{p}}$. If n is the size of $\mathbf{p}$, the traditional technique (which computes the gradient by finite differences) requires to solve the state equation (15) n times to obtain $\frac{\partial\mathcal{J}}{\partial\mathbf{p}}$: basically if p_i is the i-th component of $\mathbf{p}$ then for each i, we have to replace p_i by $p_i + \delta p_i$ and solve equation (15) to get the i-th component of of the derivative $\frac{\partial\mathcal{J}}{\partial\mathbf{p}}$. In the technique described in this section, the adjoint state equation (22) has to be solved only once to get this gradient. As the adjoint equation is usually very similar to the state equation, solving those requires basically the same amount of time which means that the computational time of estimating $\frac{\partial\mathcal{J}}{\partial\mathbf{p}}$ is divided by n.

The derivations of this section are done in the continuous case. This can also be done in the discrete case and will be the subject of a future report. But it is known that it is unadvisable to discretize the continuous adjoint equations. It is rather recommended to reestablish them from the original discretized problem to ensure the convergence of the minimization algorithm (which operates on the discrete equations) .

6 Application to the EEG and MEG inverse problems

Let us now be more specific about the measurements. As we said earlier, we measure the difference of potential at some locations $\mathbf{r}_1, \ldots, \mathbf{r}_{n_V}$ on the scalp and at a reference $\mathbf{r}_0$. Let $v_1, \ldots v_{n_V}$ be those measurements. In the EEG case, we would like our source current $\mathbf{J}^p$ to "explain" those measurements as best as possible. This means that if we compute the potential $V(\mathbf{r})$ with equation (7) or (12), we want the quantity

$$\mathcal{J}_V = \frac{1}{2} \sum_{i_V=1}^{n_V} (V(\mathbf{r}_{i_V}) - V(\mathbf{r}_0) - v_{i_V})^2, \tag{23}$$

to be as small as possible.

Similarly, in the MEG case, we measure the components of the magnetic field at some other locations $\mathbf{q}_1, \ldots, \mathbf{q}_{n_V}$ in the directions $\mathbf{d}_1, \ldots, \mathbf{d}_{n_V}$. We would like our source current $\mathbf{J}^p$ to "explain" those measurements as best as possible. Let $b_1, \ldots b_{n_B}$ be those measurements. If we compute the potential $V(\mathbf{r})$ through equation (7) or (12), and then the magnetic field through equation (11) or (14), respectively, we want the quantity

$$\mathcal{J}_B = \frac{1}{2} \sum_{i_B=1}^{n_B} (\mathbf{B}(\mathbf{q}_{i_B}) \cdot \mathbf{d}_{i_B} - b_{i_B})^2, \tag{24}$$

to be as small as possible.

In the case where we have simultaneous EEG and MEG measurements, what we call the EEG+MEG case, the goal is to find the distribution of source current that minimizes the sum $\mathcal{J}_V + \mathcal{J}_B$.

Referring to section 5, the state equation is (7) or (12), depending upon what model we choose for the conductivity.

7 The volume approach

In this section, we consider the inverse EEG, MEG and EEG+MEG problems in the case where we make no assumption on the conductivity $\sigma(\mathbf{r})$ and on the primary source current $\mathbf{J}^p(\mathbf{r})$. In fact, as we will see next, the method can be used in principle to estimate $\sigma(\mathbf{r})$ as well as $\mathbf{J}^p(\mathbf{r})$. The state equation is equation (7) together with a boundary condition on S, the boundary of Ω. In practice, Ω represents the head and part of S will contain the scalp, see figure 3. The state function is the electric potential $V(\mathbf{r})$ which satisfies the following state equation and boundary condition:

$$\left\{ \begin{array}{rcll} \nabla \cdot (\sigma \nabla V) & = & \nabla \cdot \mathbf{J}^p & \text{in} \quad \Omega \\ \dfrac{\partial V}{\partial \mathbf{n}} = \nabla V \cdot \mathbf{n} & = & g & \text{on} \quad S = \partial\Omega. \end{array} \right. \tag{25}$$

Because we assume that the primary source current is located within the brain we assume that

$$\mathbf{J}^p = 0 \quad \text{on} \quad S. \tag{26}$$

The parameter $\mathbf{p}$ is the conductivity function $\sigma(\mathbf{r})$ and the primary source current vector $\mathbf{J}^p(\mathbf{r})$. The function g defined on S is unknown; it is zero everywhere except perhaps in the neck area. In practice, its effect is neglected, i.e. we can take $g = 0$. However, for the sake of generality, it is kept in the following derivations.

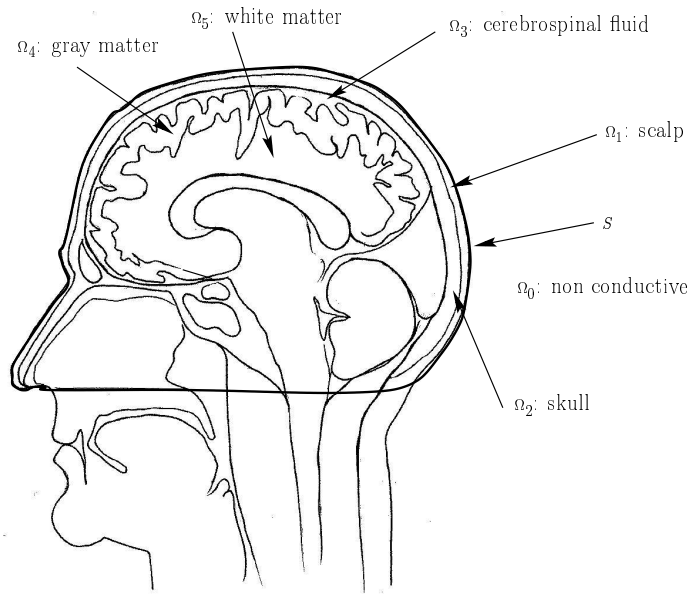

Figure 3: The various regions Ω_i. $\Omega = \Omega_1 \cup \ldots \cup \Omega_4$.

7.1 The inverse EEG volume problem

In the inverse EEG problem, we have access only to the measurements $v_{i_V}, i_V = 1, \ldots, n_{i_V}$. Therefore, we form the Lagrangian

$$\mathcal{L}_V = \mathcal{L}_V(V, w; \sigma, \mathbf{J}^p) = \mathcal{J}_V + \int_\Omega (\nabla \cdot (\sigma \nabla V) - \nabla \cdot \mathbf{J}^p)\, w\, dr\,,$$

where $w(\mathbf{r})$ is the adjoint function. In order to determine the equation it must satisfy we transform $\int_\Omega (\nabla \cdot (\sigma \nabla V) - \nabla \cdot \mathbf{J}^p)\, w\, dr$ by using the formula $\nabla \cdot (x\, \mathbf{Y}) = x\, \nabla \cdot \mathbf{Y} + \nabla x \cdot \mathbf{Y}$ (for a function x and a vector field $\mathbf{Y}$):

$$\int_\Omega (\nabla \cdot (\sigma \nabla V) - \nabla \cdot \mathbf{J}^p)\, w\, dr = \int_\Omega \nabla \cdot (w \sigma \nabla V) dr - \int_\Omega \sigma\, \nabla V \cdot \nabla w\, dr + \int_\Omega \mathbf{J}^p \cdot \nabla w dr - \int_\Omega \nabla \cdot (w \mathbf{J}^p) dr$$

We next use the formula $\int_\Omega \nabla \cdot \mathbf{X} dr = \int_S \mathbf{X} \cdot \mathbf{n}\, ds$ to transform two of the volume integrals into surface integrals:

$$\int_\Omega \nabla \cdot (w \sigma \nabla V) dr = \int_S w \sigma \nabla V \cdot \mathbf{n} ds \qquad \int_\Omega \nabla \cdot (w \mathbf{J}^p) dr = \int_S w \mathbf{J}^p \cdot \mathbf{n} ds$$

Because of our boundary condition the first integral is equal to $\int_S w \sigma g ds$ while the second one is equal to 0 as we have assumed that $\mathbf{J}^p = 0$ on S (equation (26)).

Our Lagrangian has become

$$\mathcal{L}_V = \mathcal{J}_V - \int_\Omega \sigma\, \nabla V \cdot \nabla w\, dr + \int_S \sigma\, g\, w\, ds + \int_\Omega \mathbf{J}^p \cdot \nabla w\, dr\,. \tag{27}$$

This form of the Lagrangian is suitable for computing Gateaux derivatives with respect to σ.

One more iteration of the same process on $\int_\Omega \sigma\, \nabla V \cdot \nabla w\, dr$ yields an expression for the Lagrangian that is suitable for taking Gateaux derivatives with respect to V:

$$\mathcal{L}_V = \mathcal{J}_V + \int_\Omega \nabla \cdot (\sigma\, \nabla w)\, V\, dr - \int_S \sigma V\, (\nabla w \cdot \mathbf{n})\, ds + \int_S \sigma\, g\, w\, ds + \int_\Omega \mathbf{J}^p \cdot \nabla w\, dr\,. \tag{28}$$

We impose $\nabla w \cdot \mathbf{n} = 0$ on S. The adjoint state equation is obtained by taking the Gateaux derivative of $\mathcal{L}_V$ with respect to the function $V(\mathbf{r})$:

$$\frac{\partial \mathcal{L}}{\partial V}\delta V = \sum_{i_V}(V(\mathbf{r}_{i_V}) - V(\mathbf{r}_0) - v_{i_V})(\delta V(\mathbf{r}_{i_V}) - \delta V(\mathbf{r}_0)) + \int_\Omega \nabla \cdot (\sigma \nabla w)\ \delta V\, dr$$

This must be equal to 0 for all variations δV of V, hence the adjoint state equation:

$$\boxed{\begin{cases} \nabla \cdot (\sigma \nabla w) + s_{EEG} &= 0 \quad \text{in} \quad \Omega \\ \nabla w \cdot \mathbf{n} &= 0 \quad \text{on} \quad S \end{cases}} \tag{29}$$

$$\boxed{s_{EEG}(\mathbf{r}) = \textstyle\sum_{i_V}(V(\mathbf{r}_{i_V}) - V(\mathbf{r}_0) - v_{i_V})\,(\delta(\mathbf{r} - \mathbf{r}_{i_V}) - \delta(\mathbf{r} - \mathbf{r}_0))\,,} \tag{30}$$

where $\delta(\mathbf{r})$ is the usual Dirac delta function (a distribution [43, 8]).

The G-derivative of the Lagrangian with respect to the primary source current $\mathbf{J}^p(\mathbf{r})$ is readily obtained from equation (27) since, according to equation (23), $\mathcal{J}_V$ does not contribute

$$\boxed{\frac{\partial \mathcal{L}_V}{\partial \mathbf{J}^p} = \nabla w\,.} \tag{31}$$

This equation says that in order to find the primary source current that yields a potential V that minimizes $\mathcal{J}_V$, we should follow the direction of descent $-\nabla w$ at every point $\mathbf{r}$ of the volume of interest.

As we said earlier, the method can in principle be used to estimate or refine an initial estimate of the conductivity $\sigma(\mathbf{r})$. For this purpose, we can compute the G-derivative of the Lagrangian with respect to the conductivity $\sigma(\mathbf{r})$ which is readily found from equation (27) to be equal to

$$\boxed{\frac{\partial \mathcal{L}_V}{\partial \sigma} = -\nabla V \cdot \nabla w + g(\mathbf{r})\, w(\mathbf{r}) \delta_S(\mathbf{r})\,,} \tag{32}$$

where $\delta_S(\mathbf{r})$ is the distribution such that $\int_\Omega f(\mathbf{r})\delta_S(\mathbf{r})dr = \int_S f(\mathbf{r})ds$.

7.2 The inverse MEG volume problem

In the inverse MEG problem, we have only access to the measurements b_{i_B}, therefore we form the Lagrangian

$$\mathcal{L}_B = \mathcal{L}_B(V, w; \sigma, \mathbf{J}^p) = \mathcal{J}_B + \int_\Omega (\nabla \cdot (\sigma \nabla V) - \nabla \cdot \mathbf{J}^p)\, w\, dr\,,$$

where $w(\mathbf{r})$ is, as in the previous case, the adjoint function. Just as in the previous section, we use an alternate form,

$$\mathcal{L}_B = \mathcal{J}_B + \int_\Omega \nabla \cdot (\sigma \nabla w)\, V\, dr - \int_S \sigma V\, (\nabla w \cdot \mathbf{n})\, ds + \int_S \sigma\, g\, w\, ds + \int_\Omega \mathbf{J}^p \cdot \nabla w\, dr\,,$$

of the Lagrangian to compute the adjoint state equation. It is obtained by making explicit how $\mathcal{J}_B$ depends upon the potential function $V(\mathbf{r})$. This is achieved by using equation (11) which yields the Gateaux derivative of $\mathbf{B}(\mathbf{q}_{i_B}) \cdot \mathbf{d}_{i_B}$ with respect to V:

$$\frac{\partial(\mathbf{B}(\mathbf{q}_{i_B}) \cdot \mathbf{d}_{i_B})}{\partial V}(\mathbf{r}) = \frac{\mu_0}{4\pi}\mathbf{d}_{i_B} \cdot \frac{\partial\left(\int_\Omega V(\mathbf{r}')\nabla'\sigma \times \frac{\mathbf{q}_{i_B}-\mathbf{r}'}{\|\mathbf{q}_{i_B}-\mathbf{r}'\|^3}dr'\right)}{\partial V}(\mathbf{r}) = \frac{\mu_0}{4\pi}\nabla\sigma \cdot \left(\frac{\mathbf{q}_{i_B}-\mathbf{r}}{\|\mathbf{q}_{i_B}-\mathbf{r}\|^3} \times \mathbf{d}_{i_B}\right).$$

The adjoint state equation is thus found to be

$$\boxed{\begin{cases} \nabla \cdot (\sigma \nabla w) + \nabla\sigma \cdot \mathbf{s}_{MEG} = 0 \quad \text{in} \quad \Omega \\ \nabla w \cdot \mathbf{n} = 0 \quad \text{on} \quad S\,, \end{cases}} \tag{33}$$

where

$$\boxed{\mathbf{s}_{MEG}(\mathbf{r}) = \frac{\mu_0}{4\pi}\sum_{i_B}(\mathbf{B}(\mathbf{q}_{i_B}) \cdot \mathbf{d}_{i_B} - b_{i_B})\frac{\mathbf{q}_{i_B}-\mathbf{r}}{\|\mathbf{q}_{i_B}-\mathbf{r}\|^3} \times \mathbf{d}_{i_B}\,.} \tag{34}$$

Equation (33) is very similar to equation (29), the difference being in the source term $\nabla\sigma \cdot \mathbf{s}_{MEG}$ versus s_{EEG}.

The G-derivative of $\mathcal{L}_B$ with respect to the primary source current $\mathbf{J}^p$ is seen to be equal to the G-derivative of $\mathcal{L}_V$ plus the G-derivative of $\mathcal{J}_B$ (since we have seen that $\frac{\partial \mathcal{J}_V}{\partial \mathbf{J}^p} = 0$). Equations (11) and (10) tell us that this last derivative arises from the field $\mathbf{B}_0$ and is equal to $\mathbf{s}_{MEG}$. Hence we have

$$\boxed{\frac{\partial \mathcal{L}_B}{\partial \mathbf{J}^p} = \frac{\partial \mathcal{L}_V}{\partial \mathbf{J}^p} + \mathbf{s}_{MEG} = \nabla w + \mathbf{s}_{MEG}\,.} \tag{35}$$

We can also compute the G-derivative of the Lagrangian with respect to the conductivity σ using another form of the Lagrangian, similar to (27)

$$\mathcal{L}_B = \mathcal{J}_B - \int_\Omega \sigma\, \nabla V \cdot \nabla w\, dr + \int_S \sigma\, g\, w\, ds + \int_\Omega \mathbf{J}^p \cdot \nabla w\, dr,$$

and equation (9):

$$\boxed{\frac{\partial \mathcal{L}_B}{\partial \sigma} = \frac{\partial \mathcal{L}_V}{\partial \sigma} - \nabla V \cdot \mathbf{s}_{MEG} = -\nabla V \cdot (\nabla w + \mathbf{s}_{MEG}) + g(\mathbf{r})w(\mathbf{r})\delta_S(\mathbf{r}).} \tag{36}$$

7.3 The inverse EEG+MEG volume problem

The results obtained in the previous two sections have prepared the ground for the case where we have access to simultaneous electric potential and magnetic measurements. We form the corresponding Lagrangian

$$\mathcal{L}_{V+B} = \mathcal{L}_V + \mathcal{J}_B = \mathcal{L}_B + \mathcal{J}_V = \mathcal{J}_V + \mathcal{J}_B + \int_\Omega (\nabla \cdot (\sigma \nabla V) - \nabla \cdot \mathbf{J}^p)\, w\, dr\,.$$

The adjoint state equation is

$$\left\{ \begin{array}{rcl} \nabla \cdot (\sigma \nabla w) + s_{EEG} + \nabla \sigma \cdot \mathbf{s}_{MEG} & = & 0 \quad \text{in} \quad \Omega \\ \nabla w \cdot \mathbf{n} & = & 0 \quad \text{on} \quad S\,. \end{array} \right. \tag{37}$$

We can also find the values of the G-derivatives of the Lagrangian with respect to the primary source current and the conductivity:

$$\begin{array}{rcl} \dfrac{\partial \mathcal{L}_{V+B}}{\partial \mathbf{J}^p} & = & \dfrac{\partial \mathcal{L}_B}{\partial \mathbf{J}^p} \\ \dfrac{\partial \mathcal{L}_{V+B}}{\partial \sigma} & = & \dfrac{\partial \mathcal{L}_B}{\partial \sigma}\,. \end{array}$$

7.4 Regularization of the primary source current: the volume case

The approach that we have outlined in the previous three sections can easily be extended to include regularization constraints on the primary source current $\mathbf{J}^p$ (and for that matter on the conductivity function σ, but we will not discuss this here). In particular, since noise is present in the measurements, the primary source current is likely to be noisy. One may therefore add to the Lagrangians $\mathcal{L}_V$, $\mathcal{L}_B$ or $\mathcal{L}_{V+B}$ a regularization term of the form

$$\int_\Omega \Phi(\|\nabla(\|\mathbf{J}^p(\mathbf{r})\|)\|) dr\,. \tag{38}$$

The classical choice for the function $\Phi : \mathbb{R} \rightarrow \mathbb{R}^+$ is $x \rightarrow x^2$ i.e the one related to the well-known *Tikhonov* regularization term [45]. In that case, we would be searching for the function $\mathbf{J}^p$ which will be simultaneously close to the measurements and smooth enough, since we are actually minimizing the gradient of the magnitude of the primary source current. If the function $\mathbf{J}^p$ is known to have sharp discontinuities, and this is a more realistic assumption in our application, the *Tikhonov* based regularization approach will not take care of these discontinuities and will definitely destroy this important information by isotropically smoothing the solution.

One way to prevent the destruction of such primary source current discontinuities is to choose the function Φ in such a way that the smoothing process will act isotropically in the regions with low gradient magnitude for the primary source current, and only in the direction normal to the gradient vector in the regions with a high gradient magnitude. Many functions Φ have been proposed in the literature (see [12, 2, 1, 27, 26, 28, 25]).

Once we have chosen such a function Φ, the adjoint state approach extends readily: the adjoint space equation is unchanged and it is only the derivatives of the Lagrangians with respect to the primary source current that needs to be changed to take into account the regularization term (38). Let us denote by $D\mathbf{J}^p$ the 3×3 matrix representing the derivative of the function $\mathbf{J}^p : \mathbb{R}^3 \rightarrow \mathbb{R}^3$. It is easy to show that

$$\|\nabla(\|\mathbf{J}^p(\mathbf{r})\|)\| = \frac{\|D\mathbf{J}^p \cdot \mathbf{J}^p\|}{\|\mathbf{J}^p\|}\,.$$

It is seen that this expression is a function of $\mathbf{J}^p$ and its first order derivatives $D\mathbf{J}^p$. Let us denote by $J^p_k, k = 1, 2, 3$, the three coordinates of $\mathbf{J}^p$ and rewrite $\Phi(\|\nabla(\|\mathbf{J}^p(\mathbf{r})\|)\|) = \Phi(\frac{\|D\mathbf{J}^p \cdot \mathbf{J}^p\|}{\|\mathbf{J}^p\|})$ as $F(\mathbf{J}^p, \nabla J^p_1, \nabla J^p_2, \nabla J^p_3)$. We must therefore add to the gradient of the Lagrangians which we have computed in the previous sections the vector whose kth coordinate is

$$F_{J^p_k} - \frac{\partial F_{J^p_{kx}}}{\partial x} - \frac{\partial F_{J^p_{ky}}}{\partial y} - \frac{\partial F_{J^p_{kz}}}{\partial z} \quad k = 1, 2, 3\,,$$

which can also be rewritten in a more compact form:

$$F_{J_k^p} - \nabla \cdot \frac{\partial F}{\partial(\nabla F_k^p)} \quad k = 1, 2, 3 \,.$$

7.5 A comparison with other approaches: the volume case

We do this comparison in the EEG case but it is also valid for the MEG and EEG+MEG cases. We assume that the conductivity function is known. The "traditional" inverse EEG problem is that of minimizing $\mathcal{J}_V$ with respect to $\mathbf{J}^p$ given the fact that the potential V satisfies equation (25) and is therefore, indirectly, a function of $\mathbf{J}^p$. In order to minimize $\mathcal{J}_V$ with respect to $\mathbf{J}^p$ one has to compute its gradient with respect to $\mathbf{J}^p$ and hence the gradient of V with respect to $\mathbf{J}^p$. In other words one has to solve the problem of determining how the solution of the Partial Differential Equation (25) varies when one varies $\mathbf{J}^p$ in the righthand side. This is a hard problem which should be compared to the one consisting in a) solving the adjoint state equation (29) for the adjoint state function w and b) computing its gradient ∇w since, according to equation (31), it is equal to the G-derivative of $\mathcal{J}_V$ with respect to $\mathbf{J}^p$.

8 The surface approach

This section tackles the same three problems than the previous ones but the assumptions change from the most general ones to more specific. In effect, we assume that the conductivity $\sigma(\mathbf{r})$ is constant within each region Ω_i where it is equal to σ_i. As we saw in section 3, it is sufficient to know V on the surfaces S_{ij}. The state equation (25) now becomes equation (12), V_0 being given by (13). The unknowns are the primary source current $\mathbf{J}^p(\mathbf{r})$ and possibly the n conductivities $\sigma_1, \ldots \sigma_n$. The data terms $\mathcal{J}_V$ and $\mathcal{J}_B$ are unchanged.

8.1 The inverse EEG surface problem

Similarly to the volume case, we form a Lagrangian, noted $\mathcal{L}_{V_S}$:

$$\mathcal{L}_{V_S} = \mathcal{L}_{V_S}(V, w; \sigma_1, \ldots, \sigma_n, \mathbf{J}^p) = \mathcal{J}_V + \sum_{ij} \int_{S_{ij}} \left[(\sigma_i + \sigma_j) V(\mathbf{r}) - 2\sigma_0 V_0(\mathbf{r}) - \frac{1}{2\pi} \sum_{kl} (\sigma_k - \sigma_l) \int_{S_{kl}} V(\mathbf{r}') \, \nabla' \left(\frac{1}{R} \right) \cdot \mathbf{n}_{kl}(\mathbf{r}') \, ds'_{kl} \right] w(\mathbf{r}) \, ds_{ij},$$

where $w(\mathbf{r})$ is a function that needs only to be defined on the interfaces S_{ij}. In order to obtain the adjoint state equation satisfied by w, let us expand the previous equation into

$$\mathcal{L}_{V_S} = \mathcal{J}_V + \sum_{ij} \int_{S_{ij}} \left((\sigma_i + \sigma_j) V(\mathbf{r}) - 2\sigma_0 V_0(\mathbf{r}) \right) w(\mathbf{r}) \, ds_{ij} + \frac{1}{2\pi} \sum_{ij} \sum_{kl} (\sigma_k - \sigma_l) \int_{S_{ij}} \left(\int_{S_{kl}} V(\mathbf{r}') \, w(\mathbf{r}) \, \nabla' \left(\frac{1}{R} \right) \cdot \mathbf{n}_{kl}(\mathbf{r}') \, ds'_{kl} \right) ds_{ij}.$$

Let us now switch the two summation and integral signs in the righthand side:

$$\mathcal{L}_{V_S} = \mathcal{J}_V + \sum_{ij} \int_{S_{ij}} \left((\sigma_i + \sigma_j) V(\mathbf{r}) - 2\sigma_0 V_0(\mathbf{r}) \right) w(\mathbf{r}) \, ds_{ij} + \frac{1}{2\pi} \sum_{kl} \int_{S_{kl}} \left[(\sigma_k - \sigma_l) V(\mathbf{r}') \mathbf{n}_{kl}(\mathbf{r}') \cdot \left(\sum_{ij} \int_{S_{ij}} w(\mathbf{r}) \, \nabla' \left(\frac{1}{R} \right) \, ds_{ij} \right) \right] ds'_{kl}.$$

In the second summation we exchange the indexes (k,l) and (i,j) and the variables $\mathbf{r}$ and $\mathbf{r}'$:

$$\mathcal{L}_{V_S} = \mathcal{J}_V + \sum_{ij} \int_{S_{ij}} ((\sigma_i + \sigma_j)V(\mathbf{r}) - 2\sigma_0 V_0(\mathbf{r}))\; w(\mathbf{r})\, ds_{ij} - \frac{1}{2\pi} \sum_{ij} \int_{S_{ij}} \left[(\sigma_i - \sigma_j) V(\mathbf{r}) \mathbf{n}_{ij}(\mathbf{r}) \cdot \left(\sum_{kl} \int_{S_{kl}} w(\mathbf{r}')\, \nabla' \left(\frac{1}{R} \right)\; ds'_{kl} \right) \right] ds_{ij}. \quad (39)$$

The $-$ sign arises from the fact that exchanging $\mathbf{r}$ and $\mathbf{r}'$ transforms $\mathbf{R}$ into $-\mathbf{R}$ in (1). Now that we are done with this exercise in rewriting, we can compute the Gateaux derivative of $\mathcal{L}_{V_S}$ with respect to the function $V(\mathbf{r})$:

$$\frac{\partial \mathcal{L}_{V_S}}{\partial V}\, \delta V = \frac{\partial \mathcal{J}_V}{\partial V}\, \delta V + \sum_{ij} \int_{S_{ij}} (\sigma_i + \sigma_j)\, \delta V(\mathbf{r})\, w(\mathbf{r})\, ds_{ij} - \frac{1}{2\pi} \sum_{ij} \int_{S_{ij}} \left[(\sigma_i - \sigma_j) \delta V(\mathbf{r}) \mathbf{n}_{ij}(\mathbf{r}) \cdot \left(\sum_{kl} \int_{S_{kl}} w(\mathbf{r}')\, \nabla' \left(\frac{1}{R} \right)\; ds'_{kl} \right) \right] ds_{ij}.$$

This must be equal to 0 for all variations $\delta V(\mathbf{r})$ of V and we obtain the adjoint state equation:

$$\boxed{\mathbf{r} \in S_{ij} \Rightarrow (\sigma_i + \sigma_j)\, w(\mathbf{r}) + s_{EEG}(\mathbf{r}) = \frac{\sigma_i - \sigma_j}{2\pi} \mathbf{n}_{ij}(\mathbf{r}) \cdot \left(\sum_{kl} \int_{S_{kl}} w(\mathbf{r}')\, \nabla' \left(\frac{1}{R} \right)\; ds'_{kl} \right).} \quad (40)$$

Note that the source term s_{EEG} has the same value as in the volume case and is 0 for all surfaces S_{ij} except the one corresponding to the scalp.

Next we obtain the G-derivative of $\mathcal{L}_{V_S}$ with respect to the primary source current. Since the term $\mathcal{J}_V$ does not contribute, the sole contribution comes from the term V_0 in equation (39):

$$-2\sigma_0 \sum_{ij} \int_{S_{ij}} w(\mathbf{r}) \left(\frac{1}{4\pi\sigma_0} \int_\Omega \mathbf{J}^p(\mathbf{r}') \cdot \nabla' \left(\frac{1}{R} \right) dr' \right) ds_{ij}.$$

We exchange the two integral signs and the variables $\mathbf{r}$ and $\mathbf{r}'$:

$$-\frac{1}{2\pi} \int_\Omega \mathbf{J}^p(\mathbf{r}') \cdot \left(\sum_{ij} \int_{S_{ij}} w(\mathbf{r}) \nabla' \left(\frac{1}{R} \right) ds_{ij} \right) dr' = \frac{1}{2\pi} \int_\Omega \mathbf{J}^p(\mathbf{r}) \cdot \left(\sum_{ij} \int_{S_{ij}} w(\mathbf{r}') \nabla' \left(\frac{1}{R} \right) ds'_{ij} \right) dr.$$

Therefore we obtain

$$\boxed{\frac{\partial \mathcal{L}_{V_S}}{\partial \mathbf{J}^p}(\mathbf{r}) = \frac{1}{2\pi} \sum_{ij} \int_{S_{ij}} w(\mathbf{r}') \nabla' \left(\frac{1}{R} \right) ds'_{ij}.} \quad (41)$$

The gradient of the Lagrangian with respect to the conductivities σ_i can also be computed. The term $\mathcal{J}_V$ does not contribute:

$$\boxed{\frac{\partial \mathcal{L}_{V_S}}{\partial \sigma_i} = \sum_{j \text{ adjacent to } i} \int_{S_{ij}} V(\mathbf{r}) \left[w(\mathbf{r}) - \frac{1}{2\pi} \mathbf{n}_{ij}(\mathbf{r}) \cdot \left(\sum_{kl} \int_{S_{kl}} w(\mathbf{r}')\, \nabla' \left(\frac{1}{R} \right)\; ds'_{kl} \right) \right] ds_{ij}.} \quad (42)$$

8.2 The inverse MEG surface problem

Similarly to the volume case, we form a Lagrangian, noted $\mathcal{L}_{B_S}$:

$$\mathcal{L}_{B_S} = \mathcal{L}_{B_S}(V, w; \sigma_1, \ldots, \sigma_n, \mathbf{J}^p) = \mathcal{J}_B + \sum_{ij} \int_{S_{ij}} \left[(\sigma_i + \sigma_j) V(\mathbf{r}) - 2\sigma_0 V_0(\mathbf{r}) - \frac{1}{2\pi} \sum_{kl} (\sigma_k - \sigma_l) \int_{S_{kl}} V(\mathbf{r}') \nabla' \left(\frac{1}{R} \right) \cdot \mathbf{n}_{kl}(\mathbf{r}') \, ds'_{kl} \right] w(\mathbf{r}) \, ds_{ij}.$$

$w(\mathbf{r})$ is the adjoint state function whose equation is obtained by computing the Gateaux derivative of $\mathcal{L}_{B_S}$ with respect to the potential V. We only need to compute the Gateaux derivative of the term $\mathcal{J}_B$ which is obtained through equation (14) which yields the Gateaux derivative of of $\mathbf{B}(\mathbf{q}_{i_B}) \cdot \mathbf{d}_{i_B}$ with respect to V

$$\frac{\partial (\mathbf{B}(\mathbf{q}_{i_B}) \cdot \mathbf{d}_{i_B})}{\partial V} \delta V(\mathbf{r}) = \mathbf{d}_{i_B} \cdot \frac{\mu_0}{4\pi} \sum_{ij} (\sigma_i - \sigma_j) \int_{S_{ij}} \delta V(\mathbf{r}) \mathbf{n}_{ij}(\mathbf{r}) \times \frac{\mathbf{q}_{i_B} - \mathbf{r}}{\| \mathbf{q}_{i_B} - \mathbf{r} \|} ds_{ij}.$$

This shows that the term coming from $\mathcal{J}_B$ is given by

$$\mathbf{r} \in S_{ij} \Rightarrow \frac{\mu_0}{4\pi} (\sigma_i - \sigma_j) \sum_{i_B} (B(\mathbf{q}_{i_B}) \cdot \mathbf{d}_{i_B} - b_{i_B}) \mid \mathbf{d}_{i_B} \, \mathbf{n}_{ij}(\mathbf{r}) \, \frac{\mathbf{q}_{i_B} - \mathbf{r}}{\| \mathbf{q}_{i_B} - \mathbf{r} \|^3} \mid,$$

where $\mid \mathbf{x} \, \mathbf{y} \, \mathbf{z} \mid$ is the 3×3 determinant of the three vectors $\mathbf{x}$, $\mathbf{y}$, $\mathbf{z}$. This is precisely equal to $(\sigma_i - \sigma_j) \mathbf{n}_{ij}(\mathbf{r}) \cdot \mathbf{s}_{MEG}(\mathbf{r})$. Where $\mathbf{s}_{MEG}(\mathbf{r})$ has been defined in section 7.2. The adjoint state equation is obtained

$$\boxed{\begin{array}{l} \mathbf{r} \in S_{ij} \Rightarrow \\ (\sigma_i + \sigma_j) \, w(\mathbf{r}) + (\sigma_i - \sigma_j) \mathbf{n}_{ij}(\mathbf{r}) \cdot \mathbf{s}_{MEG}(\mathbf{r}) = \dfrac{\sigma_i - \sigma_j}{2\pi} \mathbf{n}_{ij}(\mathbf{r}) \cdot \left(\displaystyle\sum_{kl} \int_{S_{kl}} w(\mathbf{r}') \nabla' \left(\frac{1}{R} \right) \, ds'_{kl} \right). \end{array}} \tag{43}$$

Next we obtain the G-derivative of $\mathcal{L}_{B_S}$ with respect to the primary source current. It is equal to the sum of the derivative of $\mathcal{L}_{V_S}$ plus the contribution of the term $\mathcal{J}_B$ which arises solely from the term $\mathbf{B}_0$ defined by equation (10). It is found to be equal to

$$\frac{\partial \mathcal{J}_B}{\partial \mathbf{J}^p}(\mathbf{r}) = \mathbf{s}_{MEG}(\mathbf{r}).$$

Therefore

$$\boxed{\frac{\partial \mathcal{L}_{B_S}}{\partial \mathbf{J}^p}(\mathbf{r}) = \frac{\partial \mathcal{L}_{V_S}}{\partial \mathbf{J}^p}(\mathbf{r}) + \mathbf{s}_{MEG}(\mathbf{r}).} \tag{44}$$

The derivatives of the Lagrangian with respect to the conductivities σ_i can also be computed. Since we saw in the previous section that the term $\mathcal{J}_V$ did not contribute, it is the sum of the derivatives of $\mathcal{L}_{V_S}$ with respect to σ_i and the derivative of $\mathcal{J}_B$ with respect to σ_i. Using equation (14), we obtain

$$\frac{\partial \mathcal{J}_B}{\partial \sigma_i} = \frac{\mu_0}{4\pi} \sum_{i_B} (B(\mathbf{q}_{i_B}) \cdot \mathbf{d}_{i_B} - b_{i_B}) \, \mathbf{d}_{i_B} \cdot \left[\sum_{j \text{ adjacent to } i} \int_{S_{ij}} V(\mathbf{r}) \frac{\mathbf{q}_{i_B} - \mathbf{r}}{\| \mathbf{q}_{i_B} - \mathbf{r} \|^3} \times \mathbf{n}_{ij}(\mathbf{r}) ds_{ij} \right],$$

which is equal to

$$- \sum_{j \text{ adjacent to } i} \int_{S_{ij}} V(\mathbf{r}) \mathbf{n}_{ij}(\mathbf{r}) \cdot \mathbf{s}_{MEG}(\mathbf{r}) ds_{ij}.$$

Therefore

$$\boxed{\frac{\partial \mathcal{L}_{B_S}}{\partial \sigma_i} = \frac{\partial \mathcal{L}_{V_S}}{\partial \sigma_i} - \sum_{j \text{ adjacent to } i} \int_{S_{ij}} V(\mathbf{r}) \mathbf{n}_{ij}(\mathbf{r}) \cdot \mathbf{s}_{MEG}(\mathbf{r}) ds_{ij}.} \tag{45}$$

8.3 The inverse EEG+MEG surface problem

To conclude this section, we go through the case where we have access to both electric potential and magnetic measurements. We form the corresponding Lagrangian

$$\mathcal{L}_{V_S+B_S} = \mathcal{L}_{V_S} + \mathcal{J}_B = \mathcal{L}_{B_S} + \mathcal{J}_V = \mathcal{J}_V + \mathcal{J}_B +$$
$$\sum_{ij} \int_{S_{ij}} \left[(\sigma_i + \sigma_j) V(\mathbf{r}) - 2\sigma_0 V_0(\mathbf{r}) - \frac{1}{2\pi} \sum_{kl} (\sigma_k - \sigma_l) \int_{S_{kl}} V(\mathbf{r}') \nabla' \left(\frac{1}{R} \right) \cdot \mathbf{n}_{kl}(\mathbf{r}') \, ds'_{kl} \right] w(\mathbf{r}) \, ds_{ij}.$$

The adjoint state equation is

$$\boxed{\begin{array}{l} \mathbf{r} \in S_{ij} \Rightarrow \\ (\sigma_i + \sigma_j) \, w(\mathbf{r}) + s_{EEG}(\mathbf{r}) + (\sigma_i - \sigma_j) \mathbf{n}_{ij}(\mathbf{r}) \cdot \mathbf{s}_{MEG}(\mathbf{r}) = \\ \qquad \qquad \frac{\sigma_i - \sigma_j}{2\pi} \mathbf{n}_{ij}(\mathbf{r}) \cdot \left(\sum_{kl} \int_{S_{kl}} w(\mathbf{r}') \nabla' \left(\frac{1}{R} \right) \, ds'_{kl} \right). \end{array}} \tag{46}$$

We also find the values of the derivatives of the Lagrangian with respect to the primary source current and the conductivities

$$\boxed{\left\{ \begin{array}{lllll} \dfrac{\partial \mathcal{L}_{V_S+B_S}}{\partial \mathbf{J}^p}(\mathbf{r}) & = & \dfrac{\partial \mathcal{L}_{B_S}}{\partial \mathbf{J}^p}(\mathbf{r}) & = & \dfrac{\partial \mathcal{L}_{V_S}}{\partial \mathbf{J}^p}(\mathbf{r}) + \mathbf{s}_{MEG}(\mathbf{r}) \\ \dfrac{\partial \mathcal{L}_{V_S+B_S}}{\partial \sigma_i} & = & \dfrac{\partial \mathcal{L}_{B_S}}{\partial \sigma_i} & = & \dfrac{\partial \mathcal{L}_{V_S}}{\partial \sigma_i} - \displaystyle\sum_{j \text{ adjacent to } i} \int_{S_{ij}} V(\mathbf{r}) \, \mathbf{n}_{ij}(\mathbf{r}) \cdot \mathbf{s}_{MEG}(\mathbf{r}) ds_{ij}. \end{array} \right.}$$

8.4 Regularization of the primary source current: the surface case

The regularization approach that has been sketched out in section 7.4 in the volume case can be extended to the surface case in a relatively straightforward fashion. We postpone a detailed discription of this extension to a future report.

9 Incorporating constraints on the primary source current

Many authors [22] have pointed out that the primary source current could be in many cases considered to be a distribution of dipoles. Most of the time there is a finite number of such dipoles which can be constrained in position, orientation or both [36, 10]. Our approach allows to introduce such constraints very naturally. For example, we may want the primary currents to be located on the cortex. We thus take

$$\mathbf{J}^p(\mathbf{r}) = \mathbf{Q}(\mathbf{r}) \delta_{S_c}(\mathbf{r}).$$

where S_c is the surface of the cortex obtained, e.g. from the segmentation of anatomical MR images. As an illustration of this, figure 4 shows a sagittal cross-section of an anatomical MR volume image of a

human head showing clearly the different anatomical regions sketched in figure 3 (and many more). Figure 5 shows a comparison, in another cross-section of the same volume, of different segmentation techniques aimed at recovering an accurate geometric description of the two surfaces (internal and external) of the cortex: referring to figure 3, these surfaces are S_{34} and S_{45}. The left column of figure 5 shows three partial cross-sections where the cerebrospinal fluid, the gray and white matter are quite visible; the second column shows the result of applying a simple threshold to the image to separate the various components; the third column shows the result of looking explicitely for the two surfaces S_{34} and S_{45} using a pair of coupled Partial Differential Equations [19]. Figure 6 shows a 3D representations of those surfaces: S_{34} is on the left, S_{45} on the right of the figure.

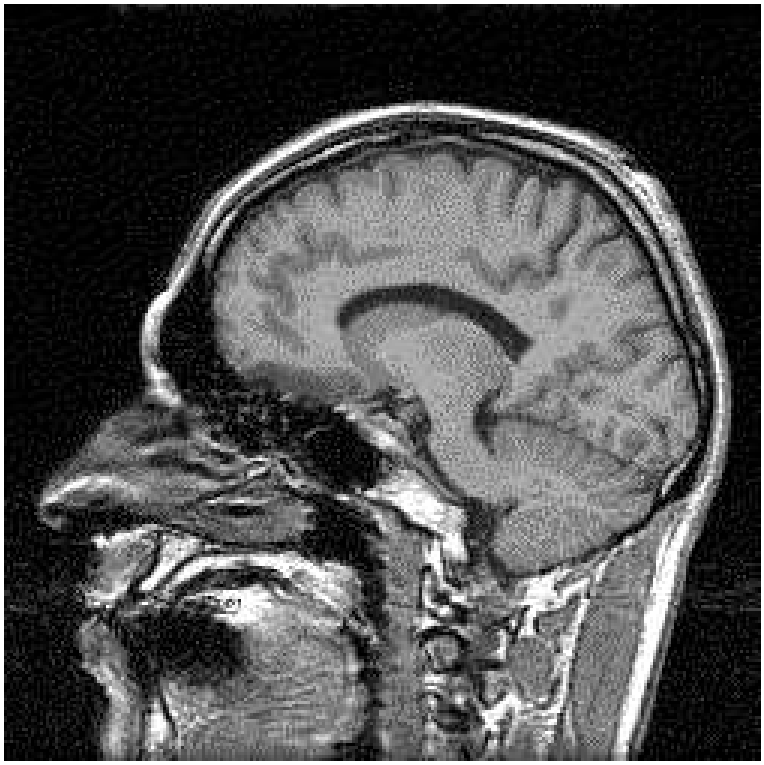

Figure 4: Sagittal cross-section of an anatomical MR volume image.

Returning to our mathematical analysis, the terms that change in the previous analysis are V_0 and $\mathbf{B}_0$ which become

$$V_0(\mathbf{r}) = \frac{1}{4\pi\sigma_0} \int_{S_c} \nabla' \left(\frac{1}{R}\right) \cdot \mathbf{Q}(\mathbf{r}') ds'$$

$$\mathbf{B}_0(\mathbf{r}) = \frac{\mu_0}{4\pi} \int_{S_c} \mathbf{Q}(\mathbf{r}') \times \nabla' \left(\frac{1}{R}\right) ds'.$$

This has only the effect of multiplying the various derivatives of the Lagrangians with respect to the primary source current by $\delta_{S_c}(\mathbf{r})$ which means that instead of having to compute a volume distribution of primary source current, we only have to compute a surface distribution of vectors.

Next we may assume that the dipoles $\mathbf{Q}$ are normal to the surface of the cortex, hence we write

$$\mathbf{J}^p(\mathbf{r}) = \lambda(\mathbf{r})\mathbf{n}(\mathbf{r})\delta_{S_c}(\mathbf{r}),$$

where $\mathbf{n}(\mathbf{r})$ is the unit normal to the surface S_c at point $\mathbf{r}$ and $\lambda(\mathbf{r})$ is the intensity of the dipole at that point. This has only the effect of having to take the dot product of the previous derivatives with the normal

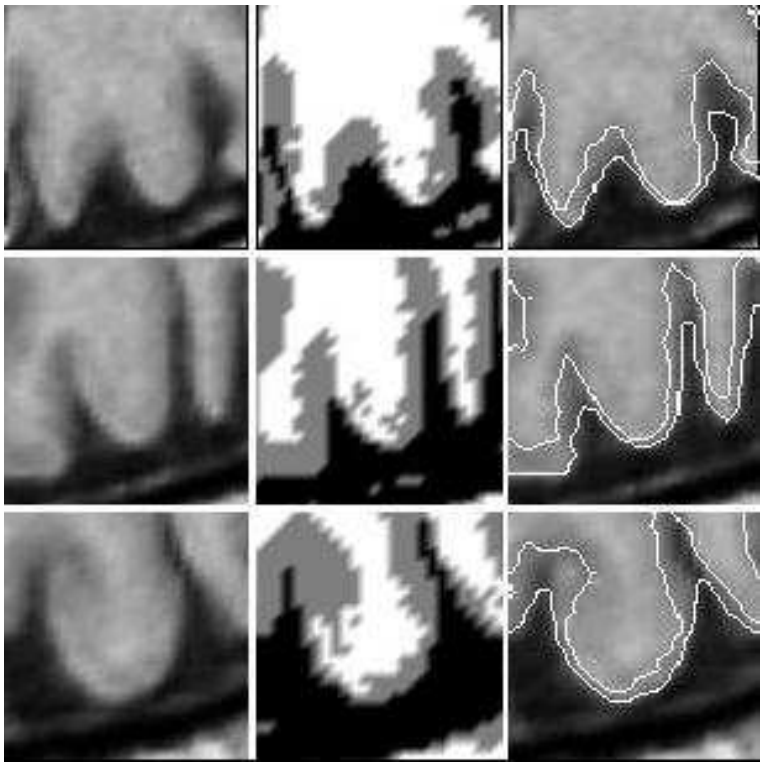

Figure 5: Finding the regions Ω_i from the MR image of figure 4.

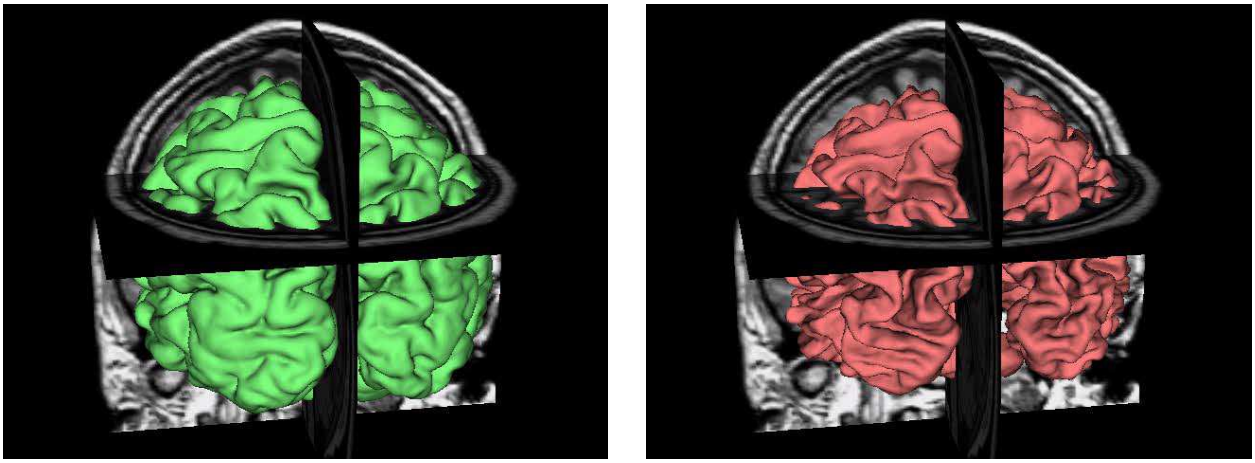

Figure 6: Left: The surface S_{34} between the cerebrospinal fluid and the gray matter. Right: The surface S_{45} between the gray and white matter.

$\mathbf{n}(\mathbf{r})$ at the point $\mathbf{r}$ of S_c. For example we have

$$\frac{\partial \mathcal{L}_{V_{S_c}}}{\partial \lambda}(\mathbf{r}) = \frac{1}{2\pi}\mathbf{n}(\mathbf{r}) \cdot \left(\sum_{ij} \int_{S_{ij}} w(\mathbf{r}') \nabla' \left(\frac{1}{R} \right) ds'_{ij} \right) \delta_{S_c}(\mathbf{r}).$$

In this particular case we only have to compute a surface distribution of scalars, i.e. a function defined on S_c.

We may also want to regularize the primary source current to reduce the effect of the noise while preserving its discontinuity which may signal some important phenomena. This is analogous to the problem of image restoration in the presence of noise and has been studied in computer vision [27]. Let us see how we can adapt this formalism to the case where we seek a function λ defined on the surface S_c. We add to the Lagrangians a regularization term of the form

$$\int_{S_c} \Phi(\|\nabla \lambda(\mathbf{r})\|) ds,$$

where $\nabla\lambda$ is the gradient of the function λ taken *on the surface*, see for example [14].

10 Conclusion

We have considered the problem of reconstructing the three-dimensional electrical activity of the brain from measurements of the electrical potential at some points on the surface of the scalp or/and from measurements of the magnetic field induced by this activity at some points around the head.

Starting from the Maxwell equations, we have justified the assumptions that allow us to assume that the electrical field induced by this activity derives from a potential field V (quasi-static hypothesis) and that the corresponding magnetic field is given by the Biot-Savart law. In this framework, two parameters are relevant: the primary source current $\mathbf{J}^p$ and the conductivity σ as functions of space. These parameters control the values of the potential V and the magnetic field $\mathbf{B}$ through a second order elliptic partial differential equation if we assume no spatial constraint on the conductivity and through a integral Fredholm equation of the second kind if we assume that the conductivity is piecewise constant.

The application of standard methods developed for the control of systems governed by such equations has led us to attack the problem of estimating the primary source current, i.e. the electrical activity of the brain, by the adjoint state method which has potentially two advantages. First it can significantly reduce the amount of computation required to obtain the 3D reconstruction and second, it naturally offers the possibility of estimating the conductivity as well.

We have also considered the problem of constraining the solutions either geometrically, using anatomical and functional data, or/and by forcing them to have sharp edges, a problem that some of us encountered in some of our previous work on image restoration. We have shown that the adjoint state method was quite suitable for taking such nonlinear constraints into account.

Much remains to be done. Our list of task includes the problems of the discretization of our equations, their implementation and testing on groundtruth data (phantoms), their comparison with other methods and their testing on real data. Taking into account the time variation is also certainly an important issue that we have not touched upon here.

Acknowledgement
We thank Mohamed Chouchane for helping us with some of the figures.

A Quasi-Static approximation of the Maxwell equations and derivation of the Biot-Savart law.

A.1 Approximations to the Maxwell equations

Two approximations of the full-fledged Maxwell equations are often useful. They are described as follows

The quasi-stationary approximation corresponds to the fact that we neglect the term $\varepsilon \frac{\partial \mathbf{E}}{\partial t}$ in the fourth Maxwell equation (3).

$$\nabla \times \mathbf{B} = \mu_0 \mathbf{J}.$$

In a passive non-magnetic medium, where $\nabla \times \mathbf{B} = \mu_0 \left(\sigma \mathbf{E} + \varepsilon \frac{\partial \mathbf{E}}{\partial t}\right)$, this assumption means neglecting $\frac{\partial \mathbf{E}}{\partial t}$ with respect to ohmic currents, i.e. $\|\varepsilon \frac{\partial \mathbf{E}}{\partial t}\| << \|\sigma \mathbf{E}\|$.

The quasi-static approximation corresponds to the fact that we neglect *both* the term $\varepsilon \frac{\partial \mathbf{E}}{\partial t}$ in the fourth Maxwell equation and the term $-\frac{\partial \mathbf{B}}{\partial t}$ in the second one which becomes:

$$\nabla \times \mathbf{E} = 0,$$

so that $\mathbf{E}$ is obtained from a scalar potential V , written $\mathbf{E} = -\nabla V$.

Following [22], let us show that, considering the average order of magnitude of the brain tissues permittivity $\varepsilon = 10^5 \varepsilon_0$ and conductivity $\sigma \simeq 0.3\,\Omega^{-1} m^{-1}$, the quasi-static approximation is valid for electromagnetic waves with time frequencies in a range of 0 to 100 Hz.

To verify this, we decompose the electric field in the Fourier domain and consider a planar wave of the form:

$$\mathbf{E}(\mathbf{r}, t) = \mathbf{E}_0(\mathbf{r})\, e^{2\pi j f t},$$

where f is the temporal frequency, and $\mathbf{E}_0(\mathbf{r})$ is a real amplitude vector not depending upon time. The *quasi-stationary* approximation, i.e. $\|\varepsilon \frac{\partial \mathbf{E}}{\partial t}\| << \|\sigma\, \mathbf{E}\|$, is thus equivalent to $\kappa = |2\,\pi\, f\, \varepsilon/\sigma| << 1$. In our case, $\kappa \simeq 2\,10^{-3}$ and the approximation is valid.

The *quasi-static* approximation is verified as follows. We let $\mathbf{E}_0(\mathbf{r}) = \mathbf{G}\, e^{2\pi j \mathbf{F}\cdot\mathbf{r}}$. $\mathbf{G}$ is a real amplitude vector and $\mathbf{F}$ a real spatial frequency vector satisfying the orthogonality condition $\mathbf{F} \cdot \mathbf{G} = 0$.

Because $\nabla \cdot \mathbf{E}_0(\mathbf{r}) = 2\pi j (\mathbf{F} \cdot \mathbf{G}) e^{2\pi j \mathbf{F}\cdot\mathbf{r}} = 0$ we obtain

$$\nabla \times \nabla \times \mathbf{E}_0(\mathbf{r}) = \nabla\left(\nabla \cdot \mathbf{E}_0(\mathbf{r})\right) - \Delta \mathbf{E}_0(\mathbf{r}) = -\Delta \mathbf{E}_0(\mathbf{r}).$$

Hence $\|\Delta \mathbf{E}_0(\mathbf{r})\| = |k| \|\mathbf{E}_0(\mathbf{r})\|$ or $\|\mathbf{F}\|^2 = \frac{|k|}{2\pi}$. The spatial wavelength magnitude $\lambda_F = \frac{1}{\|\mathbf{F}\|} = \sqrt{\frac{2\pi}{|k|}}$ is of the order of $417\,m$, negligible with respect to the head dimensions. The approximation $\nabla \times \mathbf{E} = 0$ is therefore valid.

A.2 From the quasi-static approximation to the Biot-Savart law.

The Biot-Savart law can be derived under the weaker *quasi-stationary* assumption i.e. $\frac{\partial \mathbf{E}}{\partial t} = 0$.

Thanks to the third Maxwell equation, $\mathbf{B}$ always derives from a vector potential, say $\mathbf{A}$ i.e.:

$$\nabla \cdot \mathbf{B} = 0 \Rightarrow \mathbf{B} = \nabla \times \mathbf{A} \quad \text{with} \quad \nabla \cdot \mathbf{A} = 0.$$

The second condition, called a *gauge* condition, avoids the indetermination related to the definition of $\mathbf{A}$.

If we introduce $\mathbf{A}$ in the fourth Maxwell equation:

$$\nabla \times \mathbf{B} = \nabla \times \nabla \times \mathbf{A} = \nabla\left(\nabla \cdot \mathbf{A}\right) - \nabla^2 \mathbf{A}.$$

We now use the relations $\nabla \cdot \mathbf{A} = 0$ and $\nabla^2 \mathbf{A} = \Delta \mathbf{A}$ to obtain the equation $\Delta \mathbf{A} = -\mu_0 \mathbf{J}$ whose solution satisfying $\mathbf{A}(\infty) = 0$ (no magnetic field at infinity) is given by Poisson's formula for harmonic functions ([8]):

$$\mathbf{A}(\mathbf{r}) = \frac{\mu_0}{4\pi} \int_\Omega \mathbf{J}(\mathbf{r}') \frac{dr'}{\|\mathbf{r} - \mathbf{r}'\|}.$$

Taking the curl, we obtain the Biot-Savart law

$$\mathbf{B}(\mathbf{r}) = \frac{\mu_0}{4\pi} \int_\Omega \mathbf{J}(\mathbf{r}') \times \frac{(\mathbf{r}-\mathbf{r}')}{\|\mathbf{r}-\mathbf{r}'\|^3} dr',$$

with $\frac{\mathbf{r}-\mathbf{r}'}{\|\mathbf{r}-\mathbf{r}\|^3} = \nabla' \left(\frac{1}{R}\right)$.

If in addition we consider a quasi-static approximation the current law takes the form of equation (6)

$$\mathbf{J}(\mathbf{r}) = \mathbf{J}^p(\mathbf{r}) + \sigma(\mathbf{r})\,\mathbf{E}(\mathbf{r}) = \mathbf{J}^p(\mathbf{r}) - \sigma(\mathbf{r})\,\nabla V(\mathbf{r}),$$

so that we can write the Biot-Savart law as in equation (9)

$$\mathbf{B}(\mathbf{r}) = \mathbf{B}_0(\mathbf{r}) - \frac{\mu_0}{4\pi} \int_\Omega \sigma(\mathbf{r}')\,\nabla' V \times \nabla' \left(\frac{1}{R}\right) dr',$$

with

$$\mathbf{B}_0(\mathbf{r}) = \frac{\mu_0}{4\pi} \int_\Omega \mathbf{J}^p(\mathbf{r}') \times \nabla' \left(\frac{1}{R}\right) dr'.$$

We also need a slightly different version of this equation in this paper. To get it, we make use of the formula $\nabla(\sigma\, V) = V\,\nabla\sigma + \sigma\,\nabla V$ to write:

$$-\int_\Omega \sigma(\mathbf{r}')\nabla' V \times \nabla' \left(\frac{1}{R}\right) dr' = \int_\Omega V(\mathbf{r}')\nabla'\sigma \times \nabla' \left(\frac{1}{R}\right) dr' - \int_\Omega \nabla'(\sigma V) \times \nabla' \left(\frac{1}{R}\right) dr'.$$

We then make use of the formula $\nabla \times (\sigma V \nabla \left(\frac{1}{R}\right)) = \nabla(\sigma V) \times \nabla \left(\frac{1}{R}\right)$ and of the formula $\int_\Omega \nabla \times \mathbf{X}\, dr = \int_S \mathbf{X} \times \mathbf{n}\, ds$ to transform the second integral into a surface integral

$$\int_S \sigma(\mathbf{r}')V(\mathbf{r}')\nabla' \left(\frac{1}{R}\right) \times \mathbf{n}(\mathbf{r}')ds',$$

where S is the boundary of Ω and $\mathbf{n}$ its normal. If we assume that the conductivity σ is null on S, this integral is zero.

We thus obtain

$$\mathbf{B}(\mathbf{r}) = \mathbf{B}_0(\mathbf{r}) + \int_\Omega V(\mathbf{r}')\nabla'\sigma \times \nabla' \left(\frac{1}{R}\right) dr',$$

which is the expected equation (11).

Since the surface S usually crosses the neck (see figure 3), it might be more reasonable to assume that σ is either known or unknown but non-zero on parts of S. This has the effect of adding more terms in the equations that we have derived. In this report, we assume that σ is 0 on S leaving the other cases for future research.

B Proof of equations (12) and (14)

We use Green's formula

$$\int_\Omega \left(\frac{\sigma}{R}\,\Delta' V - \Delta'(\frac{\sigma}{R})\,V\right) dr' = \int_\Sigma \left(\frac{\sigma}{R}\,\nabla' V - \nabla'(\frac{\sigma}{R})\,V\right) \cdot \mathbf{n}\, ds',$$

and the fact that $\Omega = \cup_k \Omega_k$. We decompose the first term on the lefthand side on the different volumes Ω_i:

$$\begin{aligned}
\int_\Omega \frac{\sigma}{R}\,\Delta' V dr' &= \sum_{k=1}^{n} \int_{\Omega_k} \frac{\sigma_k}{R}\,\Delta' V\, dr' \\
&= \sum_{k=1}^{n} \int_{\Omega_k} \frac{1}{R}\,\nabla' \cdot (\sigma_k \nabla' V)\, dr' \quad \text{because } \sigma_k \text{ is constant and } \Delta = \nabla \cdot \nabla \\
&= \sum_{k=1}^{n} \int_{\Omega_k} \frac{1}{R}\,\nabla' \cdot \mathbf{J}^p\, dr' \quad \text{because } \nabla \cdot (\sigma_k \nabla V) = \nabla \cdot \mathbf{J}^p \\
&= \sum_{k=1}^{n} \int_{\Omega_k} \nabla' \cdot \left(\frac{1}{R}\,\mathbf{J}^p\right)\, dr' - \sum_{k=1}^{n} \int_{\Omega_k} \nabla' \left(\frac{1}{R}\right) \cdot \mathbf{J}^p\, dr' \\
&= \sum_{k=1}^{n} \int_{S_k} \frac{1}{R}\,\mathbf{J}^p \cdot \mathbf{n}_k\, ds' - \sum_{k=1}^{n} \int_{\Omega_k} \nabla' \left(\frac{1}{R}\right) \cdot \mathbf{J}^p\, dr'.
\end{aligned}$$

The surface integrals cancel pair by pair on the corresponding surfaces since the normals are opposite. Moreover, the primary source current is null on the last surface (assumed to be the scalp). One thus obtains

$$\int_\Omega \frac{\sigma}{R}\,\Delta' V\, dr' = \int_\Omega \frac{\nabla' \cdot \mathbf{J}^p}{R} dr' = -\int_\Omega \nabla' \left(\frac{1}{R}\right) \cdot \mathbf{J}^p\, dr'.$$

We consider now the second term of the lefthand side. In each volume Ω_k σ_k is constant, hence

$$\int_{\Omega_k} -\sigma_k\, V(\mathbf{r}')\, \Delta' \left(\frac{1}{R}\right)\, dr' = 4\pi\sigma_k\, V(\mathbf{r}),$$

because $\Delta' \left(\frac{1}{R}\right) = -4\pi\delta(\mathbf{R})$, as the reader can easily verify, and one obtains

$$\int_\Omega -\sigma(\mathbf{r}')\, V(\mathbf{r}')\, \Delta' \left(\frac{1}{R}\right)\, dr' = 4\pi\sigma(\mathbf{r})\, V(\mathbf{r}).$$

We now consider the righthand side which we decompose on each surface S_k

$$\sum_k \int_{S_k} \left(\frac{1}{R}\,\sigma_k\, \nabla'_k V - \sigma_k \nabla' \left(\frac{1}{R}\right)\, V\right) \cdot \mathbf{n}_k\, ds'.$$

Since the gradient of the potential is a priori discontinuous when one goes from Ω_k to the neighbouring region Ω_l (since the conductivity is discontinuous), ∇'_k indicates that the component of the gradient along the normal $\mathbf{n}_k$ is computed at point $\mathbf{r}'_k$ of S_k as the limit

$$\lim_{\lambda \to 0^+} \frac{V(\mathbf{r}'_k) - V(\mathbf{r}'_k - \lambda \mathbf{n}_k)}{\lambda}.$$

This is not required for the term $\nabla' \left(\frac{1}{R}\right)$ which is continuous in general on S_k. Grouping pairs of terms in the previous sum, we obtain

$$\sum_{kl} \int_{S_{kl}} \left[\sigma_k \left(\frac{1}{R}\nabla'_k V - V \nabla' \left(\frac{1}{R}\right)\right) - \sigma_l \left(\frac{1}{R}\nabla'_l V - V \nabla' \left(\frac{1}{R}\right)\right)\right] \cdot \mathbf{n}_{kl}(\mathbf{r}') ds'.$$

In this equation, the normal vector $\mathbf{n}_{kl}$ points *away* from Ω_k. The terms $\sigma_k\, \nabla'_k V \cdot \mathbf{n}_{kl}$ and $\sigma_l\, \nabla'_l V \cdot \mathbf{n}_{lk}$ are respectively equal to the current going out of Ω_k and Ω_l. Their sum is therefore equal to 0 (the current density is continuous). Since $\mathbf{n}_{kl} = -\mathbf{n}_{lk}$, we have

$$\sigma_k\, \nabla'_k V \cdot \mathbf{n}_{kl} = \sigma_l\, \nabla'_l V \cdot \mathbf{n}_{kl},$$

and the corresponding terms add to 0 in the sum. We are therefore left with the second terms which we can group

$$-\sum_{kl}(\sigma_k-\sigma_l)\int_{S_{kl}} V(\mathbf{r}')\,\nabla'\left(\frac{1}{R}\right)\cdot\mathbf{n}_{kl}(\mathbf{r}')\,ds'_{kl}.$$

Note that the surface integrals are well-defined if $\mathbf{r}$ does not belong to any of the surfaces S_{kl}. But we are precisely interested, to establish equation (12), in points $\mathbf{r}$ that do belong to these surfaces. The final result will be obtained by taking a limit.

If we combine these three results we obtain

$$-\int_\Omega \nabla'\left(\frac{1}{R}\right)\cdot\mathbf{J}^p\,dr' + 4\pi\sigma(\mathbf{r})\,V(\mathbf{r}) = -\sum_{kl}(\sigma_k-\sigma_l)\int_{S_{kl}} V(\mathbf{r}')\,\nabla'\left(\frac{1}{R}\right)\cdot\mathbf{n}_{kl}(\mathbf{r}')\,ds'_{kl},$$

or

$$\sigma(\mathbf{r})\,V(\mathbf{r}) = \sigma_0\,V_0(\mathbf{r}) - \frac{1}{4\pi}\sum_{kl}(\sigma_k-\sigma_l)\int_{S_{kl}} V(\mathbf{r}')\,\nabla'\left(\frac{1}{R}\right)\cdot\mathbf{n}_{kl}(\mathbf{r}')\,ds'_{kl}, \tag{47}$$

where V_0 is the previous value.

As we said earlier, this is valid if $\mathbf{r}$ does not belong to any of the surfaces S_{kl}. Consider now the integral

$$g(\mathbf{q}) = \int_{S_{ij}} V(\mathbf{r}')\,\nabla'\left(\frac{1}{R}\right)\cdot\mathbf{n}_{ij}(\mathbf{r}')\,ds'_{ij} = \int_{S_{ij}} V(\mathbf{r}')\,\frac{\mathbf{q}-\mathbf{r}'}{\|\mathbf{q}-\mathbf{r}'\|^3}\cdot\mathbf{n}_{ij}(\mathbf{r}')\,ds'_{ij} \quad \mathbf{q}\notin S_{ij},$$

and assume $\mathbf{r}\in S_{ij}$. One can show that $\lim_{\mathbf{q}\to\mathbf{r}} g(\mathbf{q}) = -2\pi V(\mathbf{r}) + \int_{S_{ij}} V(\mathbf{r}')\,\frac{\mathbf{r}-\mathbf{r}'}{\|\mathbf{r}-\mathbf{r}'\|^3}\cdot\mathbf{n}_{ij}(\mathbf{r}')\,ds'$.

If we use this result in equation (47), we have

$$\sigma_i V(\mathbf{r}) = \sigma_0\,V_0(\mathbf{r}) + \frac{1}{2}(\sigma_i-\sigma_j)V(\mathbf{r}) - \frac{1}{4\pi}\sum_{kl}(\sigma_k-\sigma_l)\int_{S_{kl}} V(\mathbf{r}')\,\nabla'\left(\frac{1}{R}\right)\cdot\mathbf{n}_{kl}\,ds'_{kl} \quad \mathbf{r}\in S_{ij},$$

from which equation (12) results. The sum $\sum_{kl}$ is taken over all the surfaces, $\mathbf{n}_{kl}$ is the normal to S_{kl} oriented from k to l.

Let us now prove equation (14). We start with the Biot-Savard equation

$$B(\mathbf{r}) = \frac{\mu_0}{4\pi}\int_\Omega (\mathbf{J}^p - \sigma\,\nabla' V)\times\nabla'\left(\frac{1}{R}\right)\,dr',$$

which we split into a sum of integrals taken over the volumes Ω_k:

$$B(\mathbf{r}) = B_0(\mathbf{r}) - \frac{\mu_0}{4\pi}\sum_{k=1}^{n}\sigma_k\int_{\Omega_k}\nabla' V\times\nabla'\left(\frac{1}{R}\right)dr'.$$

Using the two relations $\nabla\times(V\nabla\left(\frac{1}{R}\right) = \nabla V\times\nabla\left(\frac{1}{R}\right)$ and $\int_\Omega \nabla\times\mathbf{u}dr = \int_S \mathbf{n}\times\mathbf{u}ds$ ($\mathbf{n}$ is the normal to S pointing away from Ω), we get

$$B(\mathbf{r}) = B_0(\mathbf{r}) + \frac{\mu_0}{4\pi}\sum_{k=1}^{n}\sigma_k\int_{S_k} V(\mathbf{r}')\nabla'\left(\frac{1}{R}\right)\times\mathbf{n}_k(\mathbf{r}')ds'_k,$$

and, by grouping as usual pairs of surfaces, the final result comes out easily

$$B(\mathbf{r}) = B_0(\mathbf{r}) + \frac{\mu_0}{4\pi}\sum_{kl}(\sigma_k-\sigma_l)\int_{S_{kl}} V(\mathbf{r}')\nabla'\left(\frac{1}{R}\right)\times\mathbf{n}_{kl}(\mathbf{r}')ds'_{kl}.$$

References

[1] G. Aubert, M. Barlaud, L. Blanc-Feraud, and P. Charbonnier. Deterministic edge-preserving regularization in computed imaging. *IEEE Trans. Imag. Process.*, 5(12), February 1997.

[2] G. Aubert and L. Vese. A variational method in image recovery. *SIAM J. Numer. Anal.*, 34(5):1948–1979, October 1997.

[3] Sylvain Baillet and Line Garnero. A bayesian approach to introducing anatomo-functional priors in the EEG/MEG inverse problem. *IEEE Transactions on Biomedical Engineering*, 44(5):374–385, May 1997.

[4] E. Biglieri and K. Yao. Some properties of svd and their application to digital signal processing. *Signal Processing*, 18:227–289, November 1989.

[5] J. Burger and G. Chavent. Identification de paramètres répartis dans les équations aux dérivées partielles. *R.A.I.R.O.*, 13(2):115–126, 1979.

[6] J.-P. Changeux. *Neuronal Man-The Biology of Mind.* Princeton Science Library, 1985. Reedited, 1997.

[7] D. Cohen. Magnetoencephalography: evidence of magnetic fields produced by alpha rhythm currents. *Science*, 161:784–786, 1968.

[8] R. Courant and D. Hilbert. *Methods of mathematical physics.* John Wiley & Sons, 1953.

[9] B.N. Cuffin and D. Cohen. Comparison of the magnetoencephalogram and electroencephalogram. *Electroenceph. Clin. Neurophysiol.*, 47:132–146, 1979.

[10] Anders M. Dale and Martin I. Sereno. Improved localization of cortical activity by combining eeg and meg with mri cortical surface reconstruction: A linear approach. *Journal of Cognitive Neuroscience*, 5(2):162–176, 1993.

[11] G. Demoment. Image reconstruction and restoration: Overview of common estimation structures and problems. *IEEE Transactions on Acoustics, Speech, Signal Processing*, 37:2024–2036, December 1989.

[12] R. Deriche and O. Faugeras. Les EDP en traitement des images et vision par ordinateur. Technical report, INRIA, November 1995. A more complete version of this Research Report has appeared in the French Revue "Traitement du Signal". Volume 13 - No 6 - Special 1996.

[13] Jean Dieudonné. *Éléments d'Analyse*, volume I. Gauthier-Villard, 1969.

[14] M. P. DoCarmo. *Differential Geometry of Curves and Surfaces.* Prentice-Hall, 1976.

[15] Olivier Faugeras and Renaud Keriven. Variational principles, surface evolution, pde's, level set methods and the stereo problem. *IEEE Trans. on Image Processing*, 7(3):336–344, March 1998.

[16] M. Fuchs and et al. Possibilities of functional brain imaging using a combination of meg and mrt. In C. Pantev, editor, *Oscillatory Event-Related Brain Dynamics*, pages 435–457, New York, November 1994. Plenum.

[17] L. Garnero and et al. Data operating in a PET/EEG/MRI experiment. *Human Brain Mapping*, 1:84–, 1995. Supp. 1.

[18] D. B. Geselowitz. On bioelectric potentials in an homogeneous volume conductor. *Biophysics Journal*, 7:1–11, 1967.

[19] J. Gomes and O. Faugeras. Reconciling distance functions and level sets. Technical Report 3666, INRIA, April 1999.

[20] M. Hämäläinen, H. Haario, and M. Lehtinen. Interferences about sources of neuromagnetic fields using Bayesian parameter estimation. TR TKK-F-A620, Helsinki University of Technology, 1987.

[21] M. Hämäläinen and R. Ilmoniemi. Interpreting measured magnetic fields of the brain: Estimates of current distributions. TR TKK-F-A559, Helsinki University of Technology, 1984.

[22] Matti Hamalainen, Riitta Hari, Risto J. IImoniemi, Jukka Knuutila, and Olli V. Lounasmaa. Magnetoencephalography-theory, insrumentation, and applications to noninvasive studies of the working human brain. *Reviews of Modern Physics*, 65(2):413–497, April 1993.

[23] H. von Helmholtz. über einige Gesetze der vertheilung elektrischer ströme in körperlichen leitern, mit anwendung auf die tierisch-elektrischen versuche. *Ann. Phys. Chem.*, 89, 1853.

[24] C. Koch. *Biophysics of Computation: Information Processing in Single Neurons.* Oxford University Press: New York, New York., 1999.

[25] P. Kornprobst. *Contributions à la restauration d'images et à l'analyse de séquences : Approches Variationnelles et Equations aux Dérivées Partielles.* PhD thesis, Université de Nice-Sophia Antipolis, 1998.

[26] P. Kornprobst, R. Deriche, and G. Aubert. Image coupling, restoration and enhancement via PDE's. In *International Conference on Image Processing*, volume II of III, pages 458–461, Santa-Barbara,California, October 1997.

[27] P. Kornprobst, R. Deriche, and G. Aubert. Nonlinear operators in image restoration. In *Proceedings of the International Conference on Computer Vision and Pattern Recognition*, pages 325–331, Puerto-Rico, June 1997. IEEE.

[28] P. Kornprobst, R. Deriche, and G. Aubert. Edp, débruitage et réhaussement en traitement d'image: Analyse et contributions. In *11 ème Congres RFIA*. AFCET, January 1998.

[29] P. Kornprobst, R. Deriche, and G. Aubert. Image sequence restoration : A pde based coupled method for image restoration and motion segmentation. In *Proceedings of the 5th European Conference on Computer Vision*, volume II, pages 548–562, Freibourg, Germany, June 1998.

[30] R.M. Leahy, J.C. Mosher, M.E. Spencer, M.X. Huang, and J.D. Lewine. A study of dipole localization accuracy for meg and eeg using a human skull phantom. Los Alamos Technical Report LA-UR-98-1442, Los Alamos National Laboratory, March 1998. Revision of LA-UR-97-4804.

[31] J.L. Lions. *Contrôle optimal des systèmes gouvernés par des équations aux dérivées partielles.* Dunod Gauthier-Villars, Paris, 1968.

[32] J.L. Lions and E. Magenes. *Problèmes aux limites non homogènes et applications.* Paris, Dunod, 1968. Volumes 1, 2, 3.

[33] Gildas Marin, Christophe Guerin, Sylvain Baillet, Line Garnero, and Gérard Meunier. Influence of skull anisotropy for the forward and inverse problems in EEG: simulation studies using FEM on realistic head models. *Human Brain Mapping*, 6:250–269, 1998.

[34] J.C. Mosher, M.E. Spencer, R.M. Leahy, and P.S. Lewis. Error bounds for eeg and meg dipole source localization. *Electroenceph. Clin. Neurophysiol.*, 86:303–321, 1993.

[35] John C. Mosher, Richard M. Leahy, and Paul S. Lewis. Matrix kernels for the forward problem in EEG and MEG. Technical Report LA-UR-97-3812, Los Alamos, 1997.

[36] John C. Mosher, Paul S. Lewis, and Richard M. Leahy. Multiple dipole modeling and localization from spatio-temporal meg data. *IEEE Transactions on Biomedical Engineering*, 39(6):541–553, 1992.

[37] M. Z. Nashed. Operator-theoric and computational approaches to ill-posed problems with application to antenna theory. *IEEE Transactions on Antennas Propagation*, AP-29:220–231, 1981.

[38] Jr. Orrison, William W., Jeffrey David Lewine, John A. Sanders, and Michael F. Hartshorne. *Functional Brain Imaging.* Mosby, 1995.

[39] R. D. Pascual-Marqui and et al. Low resolution electromagnetic tomography: A new method for localizing electrical activity of the brain. *International Journal of Psychophysiology*, 18:49–65, 1994.

[40] J.W. Phillips, R.M. Leahy, J.C. Mosher, and B. Timsari. Imaging neural activity using meg and eeg. *IEEE Engineering in Medicine and Biology Magazine*, 16(3):34–42, 97.

[41] M. Scherg and D. von Cramon. Evoked dipole source potentials of the human auditory cortex. *Electroencephalographic Clinical Neurophysiology*, 65:344–360, 1986.

[42] B. Scholz and G. Schwierz. Probability-based current dipole localization from biomagnetic fields. *IEEE Transactions on Biomedical Engineering*, 41:735–742, August 1994.

[43] L. Schwartz. *Théorie des distributions*. Hermann, 1957.

[44] S.L. Sobolev. *Applications de l'analyse fonctionnelle aux équations de la physique mathématique*. Léningrad, 1950.

[45] A.N. Tikhonov and V.Y. Arsenin. *Solutions of Ill-posed Problems*. Winston and Sons, Washington, D.C., 1977.

[46] Arthur Toga, editor. *Brain Warping*. Academic Press, 1998.

[47] T. Tuomisto, R. Hari, T. Katila, T. Poutanen, and T. Varpula. Studies of auditory evoked magnetic and electric responses: Modality specificity and modelling. *Nuovo Cimento*, D(2):471–483, 1983.

[48] J.E. Zimmerman, P. Thiene, and J.T. Harding. Design and operation of stable rf-biased superconducting quantum interference devices and a note on the properties of perfectly clean metal contacts. *J. Appl. Phys.*, 41:1572–1580, 1970.

Unité de recherche INRIA Sophia Antipolis
2004, route des Lucioles - B.P. 93 - 06902 Sophia Antipolis Cedex (France)

Unité de recherche INRIA Lorraine : Technopôle de Nancy-Brabois - Campus scientifique
615, rue du Jardin Botanique - B.P. 101 - 54602 Villers lès Nancy Cedex (France)
Unité de recherche INRIA Rennes : IRISA, Campus universitaire de Beaulieu - 35042 Rennes Cedex (France)
Unité de recherche INRIA Rhône-Alpes : 655, avenue de l'Europe - 38330 Montbonnot St Martin (France)
Unité de recherche INRIA Rocquencourt : Domaine de Voluceau - Rocquencourt - B.P. 105 - 78153 Le Chesnay Cedex (France)

Éditeur
INRIA - Domaine de Voluceau - Rocquencourt, B.P. 105 - 78153 Le Chesnay Cedex (France)
http://www.inria.fr
ISSN 0249-6399